

THE IMPACT OF TEMPERATURE ON THE EPIZOOTIC DYNAMICS
OF AMBYSTOMA TIGRINUM VIRUS (ATV) EPIZOOTICS IN
LARVAL SALAMANDERS (*AMBYSTOMA MAVORTIUM*)

By Kelsey E. Banister

A Thesis

Submitted in Partial Fulfillment
of the Requirements for the Degree of
Master of Science
in Informatics

Northern Arizona University

December 2021

Approved:

Joseph R. Mihaljevic, Ph.D., Chair

Crystal Hepp, Ph.D.

Jason Sahl, Ph.D.

ABSTRACT

THE IMPACT OF TEMPERATURE ON THE EPIZOOTIC DYNAMICS OF *AMBYSTOMA TIGRINUM* VIRUS (ATV) EPIZOOTICS IN LARVAL SALAMANDERS (*AMBYSTOMA MAVORTIUM*)

KELSEY E. BANISTER

Climate change could expand pathogen spatial distributions, accelerate transmission cycles, shifts host life cycles, and lead to emergence of disease in naïve host populations, all of which could have complex effects on disease. Quantitative frameworks like disease modeling are needed to improve our ability to predict the effects of climate and disease on host population dynamics. Amphibians are especially vulnerable to these changes, where populations are at risk of declining due to climate change, disease, and potential interaction between threats. Infecting salamander populations across the USA and Arizona, the effects of temperature on *Ambystoma tigrinum* virus (ATV) and the pathogen's interaction with its host are not well quantified making risk prediction difficult. We hypothesize seasonal variation in temperature and the resulting fluctuations to the host's immune system and the virus' replication rates likely play significant roles in ATV epizootics. Using mechanistic models accounting for temperature and host susceptibility, we evaluate the effects of temperature on ATV disease dynamics at two levels: within and between hosts. To evaluate the effects of dose and temperature within a host, we conducted a viral transmission experiment using larval salamanders. This allowed us to parameterize a full model exploring the effects of temperature on seasonal epizootic dynamics. Our results reveal a clear non-linear effect of temperature on mortality and shedding rates that is

likely mediated by temperature-influenced pathogen replication and host immune response, where cumulative mortality and shedding rate peak at 20°C. While an effect of temperature on average transmission rate was not observed, we show variation in host susceptibility increases with temperature. Using model simulations, we see earlier and more rapidly progressing epizootics when temperatures are fixed at 20°C. A fluctuating temperature regime under warmer early season conditions, however, predicts earlier and more rapid epizootics followed by a smaller late-season peak. Our findings demonstrate the utility of combining data and modeling techniques to better understand and forecast the effects of climate and disease on threatened host populations. Future work could link our model to projections of climate change to understand ATV risk in salamander populations in the US Southwest.

ACKNOWLEDGEMENTS

We primarily thank the Mihaljevic laboratory group, to include but not limited to Joseph Mihaljevic, Kathryn Cooney, Saikanth Ratnavale, Diego Olivo, Braden Spencer, Monica Long, Nicole Crews, and Zane Ondovcik at Northern Arizona University, for not only the major contributions they made towards the success of this project, but also for the tremendous amount of dedication, support, and guidance they provided. This project would not have been possible without such an incredible team. Laboratory experiments and testing was conducted at Northern Arizona University using the facilities at the Pathogen and Microbiome Institute, the School of Informatics, Cyber Systems, and Computing, and the animal holding and procedural areas in the Department of Biological Sciences. Whole genome sequencing was performed at the Transcriptional Genomics Research Institute (TGen North). We would like to thank the all the laboratory groups, technicians, and staff sharing these laboratories and workspaces, namely Kathleen Freel and the Hepp and Foster Lab Groups, for training, support, and assistance throughout our research. Computational analyses were run on Northern Arizona University's Monsoon computing cluster, funded by Arizona's Technology and Research Initiative Fund. We also thank Arizona Forest Service and the Arizona Department of Game and Fish, particularly the Ranid Frogs Project (Audrey Owens, Cody Mosley, and Maddy Marsh), for permitting, training, support, and ongoing collaborations on ranavirus and amphibian projects. Furthermore, we thank the graduate committee that provided their wealth of knowledge as well as their invaluable direction and support throughout this project: Joseph Mihaljevic, Crystal Hepp, and Jason Sahl.

TABLE OF CONTENTS

CHAPTER ONE: A review of the impacts of climate change on the disease dynamics of Ambystoma tigrinum virus.....	1
CHAPTER TWO: Modeling the within- and between-host effects of temperature on ATV infection dynamics and seasonal epizootics.....	8
INTRODUCTION.....	8
METHODS.....	10
1. Lab Experiment.....	10
<i>Overview.....</i>	10
<i>Experimental design.....</i>	11
<i>Measuring shedding rates.....</i>	13
<i>Viral quantification.....</i>	13
<i>Viral Isolation.....</i>	14
2. Full SIVR Model.....	15
3. Within Host Model.....	16
4. Epizootic Model (Between-Host Model).....	18
5. Fitting Within Host Model to Data.....	20
6. Estimating Transmission Rates.....	23
7. Simulating the Full Model Under Climate Conditions.....	24
RESULTS.....	25

1. Lab Experiment.....	25
<i>Cumulative Mortality</i>	25
<i>Shedding Rate</i>	27
2. Fitting Within Host Model to Data.....	28
<i>Cumulative Mortality</i>	28
<i>Shedding Rate</i>	31
3. Estimating Transmission Rates.....	31
4. Simulating the Full Model Under Climate Conditions	33
<i>Fixed Temperatures</i>	33
<i>Effects of Density</i>	33
<i>Fluctuating Temperature Regimes</i>	33
DISCUSSION	37
REFERENCES	45

LIST OF TABLES

Table 1: Parameter Estimates.....	29
-----------------------------------	----

LIST OF FIGURES

Figure 1: Experimental Design	11
Figure 2: SIRV model.....	15
Figure 3: Model Fit to Data	26
Figure 4: Average Shedding Rate.....	27
Figure 5: Parameter Estimates	30
Figure 6: Estimating Transmission Rate.....	32
Figure 7: Effects of Fixed Temperatures and Density on Epizootics	35
Figure 8: Simulating Fluctuating Temperatures Regimes	36

CHAPTER ONE: A review of the impacts of climate change on the disease dynamics of

Ambystoma tigrinum virus

Increasingly severe weather patterns can lead to significant changes in disease dynamics triggering detrimental cyclical outbreaks (Altizer et al., 2006, 2013; Grassly & Fraser, 2006). Emerging pathogens may rapidly spread throughout populations, infecting naive hosts (Altizer et al., 2013; Lips et al., 2008). Over time, recurrent epizootics can occur, characterized by large peaks of infection followed by periods of low transmission between events (Altizer et al., 2006, 2013; Hudson et al., 2002). While human diseases, such influenza, are notorious for such recurrent outbreaks, a large number of wildlife diseases display similar cyclical seasonal dynamics (Altizer et al., 2006; Hudson et al., 2002). These temporally variable transmission rates can be driven by seasonal fluctuations in host demography, life history, and abiotic conditions, such as temperature or precipitation (Altizer et al., 2006; Dowell, 2001).

Since environmental conditions can directly impact pathogen biology, they also influence host susceptibility to infection (Martinez, 2018). Seasonal changes can leave hosts vulnerable to disease through a decrease in host immune response and increase infection susceptibility. Unlike mammals, the internal regulation of ectothermic species is heavily dependent on environmental temperatures (Lips et al., 2008; Martinez, 2018). As a result, amphibians undergo seasonal fluctuations in body temperature and, consequently, immune response which makes them especially susceptible to disease (Raffel et al., 2006). However, the mechanisms that drive inter-annual variability in seasonal disease outbreaks are poorly understood, therefore, we propose using an environmentally sensitive amphibian-pathogen system as our model of study (Keeling & Rohani, 2007).

Amphibians are currently the most vulnerable vertebrate taxa, where more than 32% of species are threatened or endangered and over 43% are experiencing population decline (Rohr et al., 2008). A major threat to amphibian species are *Ranaviruses*, a genus of large (120-300 nm diameter) icosahedral viruses belonging to the *Iridoviridae* family with linear, double stranded DNA genomes known for their recombinant nature (Chinchar, 2002, Vilaça et al., 2019). This diverse group of viruses infects over 175 ectothermic species globally and can cause massive die-off events that impact both wild and commercial populations (Chinchar, 2002; Duffus et al., 2015). Transmission occurs during contact with free-floating virions shed from the skin of an infected individual into the environment or through physical contact (Brunner et al., 2005; Gray & Chinchar, 2015). The resulting infection is characterized by systemic disease that especially affects ectothermic species in larval life stages, which may include symptoms such as: lethargy, edema, emaciation, ulcers and lesions, hemorrhaging, and necrosis of internal organs and limbs (Chinchar, 2002; Gray & Chinchar, 2015). In North America, the two most common and well established *Ranavirus* species are frog virus 3 (FV3) and *Ambystoma tigrinum* virus (ATV) (Chinchar, 2002; Duffus et al., 2015; Epstein & Storfer, 2015). ATV has historically been found to only infect salamanders and newts (i.e., urodeles), while FV3 can infect a variety of taxonomic groups, including amphibians, reptiles, turtles, and fish (Chinchar, 2002; Duffus et al., 2015).

Interestingly, while genetically distinct and phenotypically diverse isolates of ATV and FV3 exist across the North America, variation in the average infectious period and transmission may even occur in the same region (Epstein & Storfer, 2015; J. K. Jancovich et al., 2003). The

pathogen's prevalence across a wide range of landscapes, seasonally recurrent outbreaks, and unique pathology makes this an ideal study system to explore disease dynamics and conservation (Hoverman et al., 2012; Tornabene et al., 2018). Here we focus on ATV due to its presence in Arizona, abundant salamander host populations, significant knowledge gaps, and critical conservation implications for the federally endangered Sonoran barred tiger salamander, *Ambystoma mavortium stebbinsi* (J. Collins et al., 1988; J. P. Collins & Snyder, 2002; J. Jancovich et al., 1997; J. K. Jancovich et al., 2003).

Reoccurring epizootics of ATV have been observed in *Ambystoma mavortium* populations in Southern Arizona as early as 1985 (J. Collins et al.). These decimating outbreaks were originally attributed to bacterial infections despite being unable to identify the causative agent (J. Collins et al.). However, when a similar disease was reported in threatened salamander populations in 1995, a virus was isolated and determined to be the pathogen primarily responsible for the epizootic events detected statewide (J. Jancovich et al., 1997). Despite the continued detection of ATV across Arizona and North America, the factors that drive ATV transmission remain poorly understood, with few papers published on the topic. Studies relating to ATV transmission are limited to an experiment analyzing density-dependent transmission mechanisms of ATV (Greer et al., 2008), an experiment conducted to evaluate the effects of temperature on the proportion of infected individuals and mortality rate (Rojas et al., 2005), and a study that worked to quantify the temporal and spatial dynamics of ATV epizootics in the field (Greer et al., 2009).

Nonetheless, most ATV-induced die-offs in the field are not well described and no parameterized epidemiological models have been published for ATV (J. Collins et al., 1988). In order to answer broad questions about viral transmission in both disease ecology and our study system, we will

focus on within season dynamics and improving our understanding of what parameters influence ATV transmission during epizootics.

Despite variability across species and strains, many ranaviruses, such as FV3 and common midwife toad virus (CMTV), and are highly transmissible (i.e., probability of infecting a salamander given exposure to small doses) leading to devastating die-off events where disease development in hosts may occur mere hours after infection (Robert et al., 2011). Experimental studies show that ATV has an especially high transmission rate, where a second of skin-to-skin contact with a contagious individual may lead to infection in a healthy host (Brunner et al., 2005; Gray & Chinchar, 2015). Consequently, ATV infected larval salamanders typically die around two weeks post exposure (Rojas et al., 2005). Given this information, we might expect epizootics to occur rapidly, peaking earlier in the year with high infection and mortality rates. FV3 epizootics in wood frogs show high transmission rates producing peak prevalence near 100% early in the season (Hall et al., 2018). ATV epizootics in the field, however, typically peak in the late summer and early fall with lower-than-expected prevalence (<60%) and longer-than-expected outbreaks; yet pathogen presence may be detected as early as salamander breeding season in spring (Greer et al., 2009). While it is unclear what mechanisms might influence ATV transmission and explain this observed delayed peak in prevalence and weaker epizootic, we hypothesize that variation in temperature and a host's susceptibility to infection may play significant roles in ATV epizootics.

Smaller than expected epizootics may occur when relatively resistant individuals are present in a population of high susceptible heterogeneity (Dwyer et al., 1997) and experimental data from

FV3 indicates variation in temperature may lead to changes in disease pathology. Therefore, to explain this variation in epizootics, we hypothesize that the relationships between temperature and both mortality and shedding rates are non-linear, where the trade-offs between pathogen replication and host immune response mediate the relationship. Specifically, both viral replication and the host immune system have an ideal temperature range in which functionality is optimal for reproduction or response. For example, the optimal replication temperatures for FV3 can range from 15 to 31°C, where optimal temperatures in cell culture typically range around 26°C (Ariel et al., 2009). On the other hand, evidence suggests that ATV has a preferred optimal replication range at lower temperatures averaging around 18°C (J. Jancovich et al., 1997; Rojas et al., 2005). We also expect that immune function and temperature to have a high functioning peak at intermediate temperatures and low functioning towards the low and high extremes (Lafferty & Mordecai, 2016). Whereas we typically see an increase in host immune response, such as increased phagocyte activity, at higher temperatures (Allender et al., 2013; J. K. Jancovich & Jacobs, 2011) and waning resistance to infection during colder seasons (Brand et al., 2016; Raffel et al., 2006). As a result, we expect a hump-like relationship about these optimal thermal ranges for viral replication and immune response (Lafferty & Mordecai, 2016). As environmental temperatures reach the limits of or exceed the optimal thermal ranges for viral replication or immune response, functionality and productivity decrease significantly from the mean. This interaction between the immune system and the virus may partially explain why the limited data on the effects of temperature on ATV dynamics instead suggests that intermediate temperatures result in higher mortality rates (Rojas et al., 2005). In contrast, increasing water temperatures have subsequently been linked to increases in mortality (Brand et al., 2016) and the decay of free-floating virions (Brunner & Yarber, 2018) for FV3. Therefore, the outcomes of

infection depend on this balance between viral replication, immune system functioning, and the temperature of the environment.

Given this relationship, we expect a significant decrease in ATV transmission and mortality due to lower viral replication rates with the cooler spring temperatures during the early season (Raffel et al., 2006; Rojas et al., 2005). As temperatures increase later in the season, we expect both higher immune functioning and an increase in viral replication (Raffel et al., 2006). However, as the epizootic peaks near the hottest times of the year, we also expect viral replication to begin to decrease as the upper temperature thresholds for ATV are met (Ariel et al., 2009; Brand et al., 2016). As a result, we predict that transmission rates will continue to increase with temperature across the epizootic season yielding peak mortality rates at intermediate temperatures, which may explain an epizootic period that persists longer-than-expected.

Using mechanistic models, we can evaluate the effects of temperature on ATV disease dynamics at two levels: within and between hosts. First, we will consider how the pathogen interacts with an infected host's immune system which will ultimately determine the amount of the pathogen shed into the system and the fate of the host as a result of the struggle between the immune system and viral replication. Next, we will consider the amount of virus shed back into the environment by these infectious hosts and how that influences transmission between other susceptible hosts in the population (Brand et al., 2016). We develop a model that accounts for how variability in temperature not only affects the infection progresses but host susceptibility and transmission in a population. These computational and mathematical models are then used to predict the size of epidemics. We initially conducted a carefully designed laboratory based viral

transmission experiment to evaluate the effects of dose and temperature on a single host epidemic. From this experimental data we estimate the ideal parameter ranges across temperature treatments to describe the observed relationship between temperature and within-host dynamics. This enabled us to implement statistical models to fit within and between-host models to the experimental data. This allowed us, for the first time, to parameterize a full model to explore the effects of environmental temperature on seasonal epizootic dynamics from the ground up (i.e., from within- to between-host dynamics)

CHAPTER TWO: Modeling the within- and between-host effects of temperature on ATV infection dynamics and seasonal epizootics

INTRODUCTION

Increasingly severe weather patterns have been linked to the disruption of natural populations (Altizer et al., 2006, 2013; Grassly & Fraser, 2006), dramatically affecting reproductive success and survival of wildlife populations (Altizer et al., 2013). It has been hypothesized that increasing temperatures could affect pathogen virulence leading to significant changes in disease dynamics in a changing climate (Altizer et al., 2006, 2013; Grassly & Fraser, 2006). Quantitative frameworks like disease modeling are needed to improve our ability to predict the effects of climate and disease on host population dynamics. Amphibians are especially vulnerable to these changes, where populations are at risk of declining due to climate change, disease, and potential interaction between threats (Altizer et al., 2013; Hudson et al., 2002). Over time, recurrent epizootics can occur, characterized by large peaks of infection followed by periods of low transmission between events (Altizer et al., 2006, 2013; Hudson et al., 2002). Seasonal fluctuations in host populations, such as host demography, life history, and abiotic conditions, such as temperature or precipitation can leave hosts especially vulnerable to disease (Altizer et al., 2006; Dowell, 2001). Populations experiencing warming or fluctuating seasonal temperatures may also experience an increase in infection susceptibility, immune response, and variation in these traits. Since amphibians undergo seasonal fluctuations in body temperature, they consequently experience more dramatic thermal-based shifts in immune response and behavior than mammals (Raffel et al., 2006).

Amphibians, one of the most vulnerable vertebrate taxa, can experience population declines due to both climate change and disease (Rohr et al., 2008). One such emerging pathogen is *Ambystoma tigrinum* virus (ATV) which as a member of a highly virulent genus of viral pathogens that infect amphibians, fish, and reptiles (Chinchar, 2002; Gray & Chinchar, 2015; J. Jancovich et al., 1997). While ATV has only been observed to infect salamanders (*Ambystoma mavortium* or *Ambystoma tigrinum*) in nature, experimental studies show that ATV has an especially high transmission rate, where a second of skin-to-skin contact is enough exposure to lead to infection (Brunner et al., 2005; Gray & Chinchar, 2015). However, ATV epizootics in the field, however, typically peak in the late summer and early fall, yet pathogen presence may be detected as early as salamander breeding season in spring (Greer et al., 2009). Given the high expected transmission rates for ATV, this data deviates from the rapid epizootics expected to peak early in the season with high infection and mortality. We hypothesize that variation in temperature and a host's susceptibility to infection may play significant roles in ATV epizootics. Studies show that smaller than expected epizootics may occur when relatively resistant individuals dominate the population and variation in temperature may lead to variation in susceptibility mediated by trade-offs in the optimal thermal ranges for host immune system and viral replication (Brand et al., 2016; Dwyer et al., 1997). Experiments have suggested that an increase in temperature may lead to increased viral replication and mortality but will also show increases in decay rate of free-floating virions and host immune response. Therefore, we expect the relationships between mortality and shedding rates and temperature to be non-linear, where the trade-offs between pathogen replication and host immune response mediate the relationship. Combining the various effects of temperature on host-pathogen interactions to predict how

seasonally fluctuating temperatures impact epizootics is nearly impossible without the use of quantitative modeling. Using mechanistic models, we can evaluate the effects of temperature on ATV disease dynamics at two levels: within and between hosts. Here, we develop a model that accounts for how temperature affects infection dynamics within individual hosts, as well as the spread of the virus among host individuals. These computational and mathematical models are then used to predict the size of epidemics under various environmental temperature regimes. We first conducted a carefully designed laboratory based viral transmission experiment to evaluate the effects of dose and temperature on a single host epidemic. This enables us to fit the within and between-host models to the experimental data, leading to a fully parameterized and fine-tuned model. Thus, for the first time, we have produced a fully parameterized model to explore the effects of environmental temperature on seasonal ATV epizootic dynamics from the ground up (i.e., from within- to between-host dynamics).

METHODS

1. Lab Experiment

Overview

We conducted a laboratory experiment to quantify the effects of temperature on various processes that describe interactions between ATV and its salamander host. This experiment was specifically designed to allow us to parametrize a model that describes the effects of temperature on within-host dynamics of infection as well as seasonal patterns of population-wide epizootics (i.e., between-host transmission dynamics; see model description below). In brief, we conducted a dose-response experiment by exposing larval salamanders to one of four doses of the virus while individuals were held at one of three temperatures. This allowed us to quantify how

environmental temperature affects: the average transmission rate, the variation in transmission rate among host individuals, the virus-induced mortality rate, and the rate of virus shedding from individuals.

Experimental design

To prepare for the experiment, we collected *A. mavoritium* egg masses from six sites in Coconino County, Arizona known to be ATV-free in 2018. The outer membrane of the egg masses was surface decontaminated with a low-concentration bleach solution and rinsed thoroughly with deionized (DI) water to remove any potential virions or other infectious agents present. Hatchlings were batch-reared in 40-liter containers at room temperature. Group housing was organized by site and size in order to allow for a minimum of one liter per individual. We

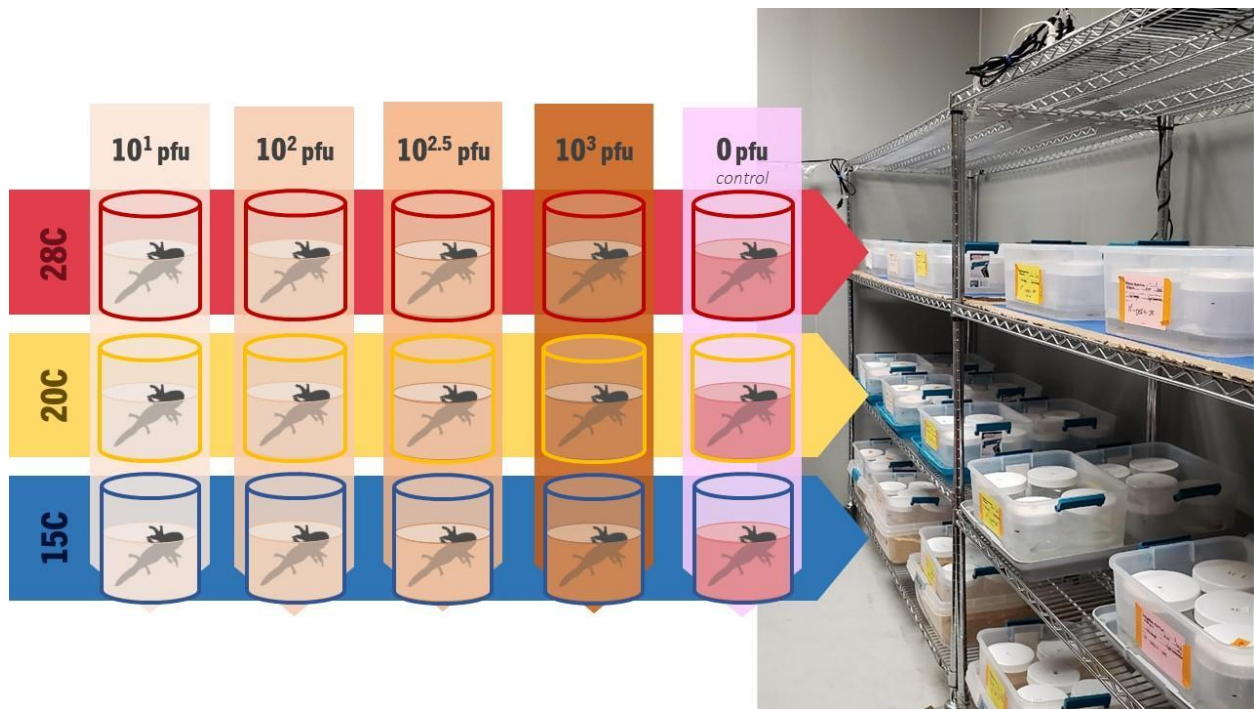


Figure 1: Experimental Design

The diagram on the left describes the design of our viral transmission experiment, such that each individual is randomly divided into different temperature (15°C, 20°C, and 28°C) – dose (10^1 , 10^2 , $10^{2.5}$, and 10^3) treatments. The image on the right shows how this experimental setup was translated in the lab.

divided the experiment into two rounds for logistical feasibility and space limitations. The first (N=164) and second (N= 127) rounds of the experiment began roughly 60 and 90 days of age respectively.

To begin the experiment, individuals were placed into separate 1L plastic containers filled with 800mL of sterile water. Each container was sealed with a screw-top lid, which could be loosened halfway to provide sufficient oxygen exchange, temperature retention, and a barrier for contamination prevention. To mimic a temperature range commonly experienced in Arizona, we randomly assigned salamanders to either 15°C, 20°C (the temperature of the room), or 28°C. holding temperatures. To maintain these temperatures, up to five of the 1L plastic containers were secondarily contained within a 12.5L opaque plastic storage container. Each secondary container was filled partially with water to prevent temperature fluctuations and gradients within individual containers. The use of waterproof seedling heating pads under the secondary containers allowed us to achieve the 28°C treatment temperatures. To maintain 15°C temperatures, the secondary containers were placed in a tertiary container containing frozen water bottles submerged in sawdust. This method granted us replicated blocks of larvae at specified water temperatures. Individual larval salamanders were allowed to acclimate to a randomly assigned treatment temperature for one week prior to virus exposure.

After acclimation, individuals were exposed to one of four different doses of ATV (10^1 , 10^2 , $10^{2.5}$, and 10^3 plaque-forming-units (PFU) per milliliter) (see viral isolation). Sham-infected (control) individuals (round one N= 14, round two N = 17) at each temperature were passively exposed to an aliquot of virus-free cell culture media, which allowed us to confirm no cross-

contamination occurred between treatments. To inoculate the salamanders, each was placed in a new container filled with 200mL of fresh, sterile water. The appropriate volume of viral medium was added to the water to reach the desired final viral concentration. Salamanders were held in these containers for a three-day exposure time. To ensure the exposure time was stopped, individuals were rinsed to remove any virus from the skin then placed into a clean container containing 800mL of temperature-appropriate DI water. Mortality events and any observed symptoms were recorded twice per day for the 35-day duration each round of the experiment. We conducted full water changes every 3-4 days per individual to maintain water quality. After the 35-day period, all remaining larvae were euthanized and stored at -20°C for later viral testing

Measuring shedding rates

To measure the viral shedding rate, 4-8 individuals were randomly selected from each temperature-dose treatment every 48 hours. Selected individuals were moved into a new container with 800mL of sterile temperature-appropriate water. After shedding into the water for a 24hr period, a 50mL aliquot of water was collected from the salamander's container and immediately frozen at -20°C. Water samples were later filtered in a biosafety cabinet using 0.22µm Polyethersulfone filters then split in half, where one half was stored at -70°C and the other was tested to determine the amount of virus shed into the water by that individual during a 24hr period. DI water controls were filtered at the start of each filtration round and after every 5-10 samples.

Viral quantification

Water filters used to estimate viral shedding were extracted using a Qiagen 96-well garnet PowerBead DNA Plates (Qiagen, Germantown, MD. USA), a MagMAX DNA Multi-Sample Ultra 2.0 extraction kit, and the KingFisher Flex Magnetic Particle automated extraction

instrument (Thermo Fisher Scientific, Waltham, MA. USA). We used the protocol listed for the half-volume MagMAX DNA Multi-Sample Ultra 2.0 extraction kit by ThermoFisher apart from the initial lysis steps. Instead, we added lysis buffer and proteinase K to each well of the PowerBead plates containing filters and empty well controls, incubated at 65°C for 5 minutes, allowed to cool for 2 minutes, and then homogenized the samples using a GenoGrinder Mini at 5000rpm for 20 minutes. To calculate the number of virions shed from the skin per individual per 800mL water per day, quantitative PCR (qPCR) assays were performed on the samples using primers targeting a 97bp segment of the major capsid protein gene (MCP) and an MGB Eclipse probe (Stilwell et al., 2018). Assays were performed following the protocol developed by Stilwell in 2018 on a QuantStudio™ 7 Flex Real-Time PCR System (ThermoFisher) using PrimeTime® Gene Expression Master Mix (Integrated DNA Technologies). To confirm viral infection, liver, kidney, and spleen samples were collected from each larva and homogenized using a motorized microcentrifuge tube pestle. DNA was extracted using a non-modified half-volume MagMAX DNA Multi-Sample Ultra 2.0 extraction kit and protocol by ThermoFisher and quantified using the Qubit 4.0 (Thermo Fisher Scientific, Waltham, MA. USA). Viral presence was determined by performing qPCR using the same methods as described for the shedding analysis. If viral presence was detected using qPCR, we then calculated the viral DNA copies per sample for further analysis.

Viral Isolation

ATV was isolated from larval *A. mavortium* tissue samples collected from a die-off event that took place at a stock-tank in Tonto National Forest, Arizona. Ranavirus presence was confirmed via qPCR using the previously mention methods and then species was confirmed via whole-genome sequencing using an Illumina MiSeq instrument with an NGS Kapa HyperPrep kit and a

MiSeq Reagent Kit Nano v2 (300-cycles) following manufacturer protocols. We subsequently passed ATV in fathead minnow (FMH; ATCC CCL-42) cells cultured in Eagle's minimum essential medium (MEM; Gibco) supplemented with 10% fetal bovine serum (FBS) and 1% penicillin-streptomycin-neomycin (PSN) antibiotics in 175cm² flasks at 20°C (Jancovich & Jacobs, 2011). Experimental data has shown that ATV can replicate at temperatures ranging from 10 to 31°C in cell culture (Jancovich et al., 1997). The final ATV stock used to inoculate the larval salamanders for the experiment was passed in FHM cells no more than 5 times and viral titer was confirmed by plaque assay in FHM cells.

2. Full SIVR Model

To explain how temperature impacts salamander-ATV interactions and epidemic dynamics, we begin with a modified version of the classic SIR model (Fig. 2). Our model includes the three standard classes, susceptible individuals (*S*), infectious individuals (*I*), and removed individuals

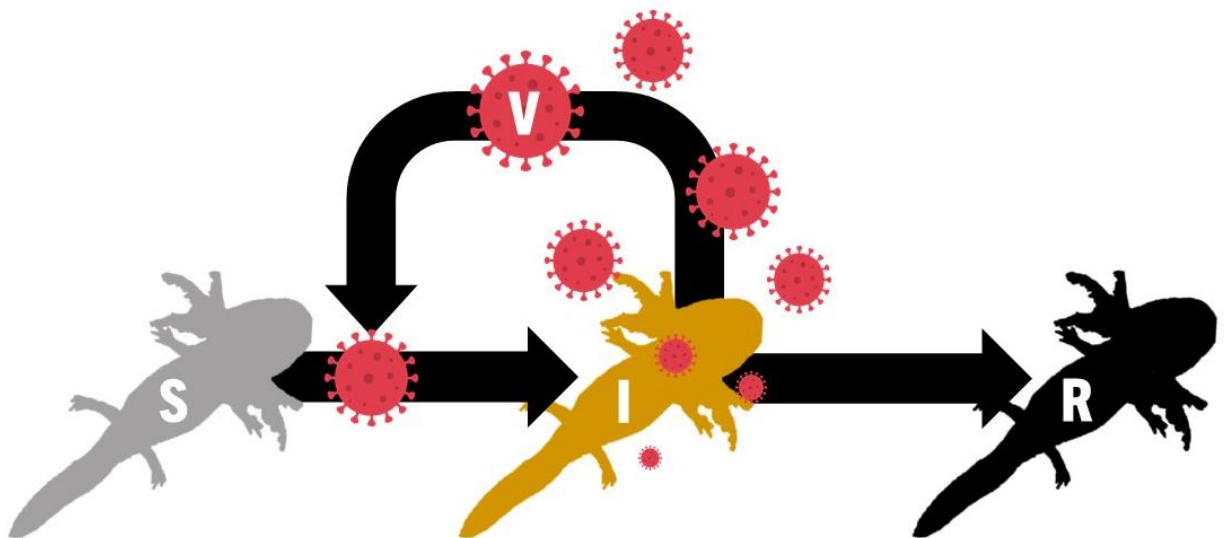


Figure 2: SIRV model

The movement of individuals between susceptible(*S*), infectious(*I*), and removed(*R*) classes where the class representing virus shed back into the environment by infectious individuals (*V*) influences transmission and the subsequent movement of individuals from the *S* to *I* classes.

(R). This system, however, includes a fourth class that explicitly tracks the density of virus (V) in the water. Our model allows for susceptible individuals to vary in their susceptibility to the virus, such that some individuals are more resistant than others. Over time, we expect individuals to move from the susceptible class to the infectious class. The infectious individuals are defined as those who have become infected by the virus and can spread the virus to susceptible individuals via viral particles shed into the environment. Infected individuals may be removed from the system by either recovery (clearance of the virus) or death. Environmental virus is defined by the total density of virus present in the aquatic environment in which the salamander population resides. Infectious individuals contribute to the V class by the amount of virus shed from their bodies. Therefore, as the infectious population increases, so does the concentration of virus in the environment which influences the chance of infecting susceptible individuals. Removed individuals are those who have been removed from the system either by recovering from the virus and are assumed to be immune or have died.

We expect that temperature regulates the interactions between the host's immune system functioning and viral replication within the host, which ultimately determines how much virus is shed from the host at any given time. We break our model down into temperature-controlled processes that occur within the host and temperature-controlled processes that determine transmission and viral decay in the environment (among-host epizootic model).

3. Within Host Model

Our analysis begins with a mechanistic model for describing within-host dynamics defined by Mihaljevic et. al (2019). Briefly, their model explains how viral replication is mediated by the

host's innate immune response. The production of immune components, Z , responds to viral infection following the Michaelis-Menten equation for a single enzyme catalyzed reaction (Johnson & Goody, 2011; Rosenbaum & Rall, 2018):

$$Z' = (N_Z - Z\delta_{(t)}) + \psi_{(t)}Z \left(\frac{V_w}{V_w + \gamma_{(t)}} \right),$$

where $Z' = \frac{dZ}{dt}$. Implicit in this model formulation is the assumption that there is a base-line density of immune components that is regulated by the function $N_Z = \delta Z(0)$, allowing the immune system to reach a stable state when no virus is present. Therefore, N_Z represents the immune component constant rate of production, and δ , the background loss of the immune components. The growth rate of the immune component in response to the within-host density of virus (V_w) is defined ψ which is mediated by γ , the half-saturation constant. In essence, the immune system ramps up in response to virus replication, but there can be a delay such that the virus must reach a certain point before the immune system detects viral growth and ramps up immune production.

Virus replication, and the interaction between the virus and host's immune system is then modeled by assuming that the virus population replicates exponentially inside the host, but that the virus' rate of growth is modulated by the immune system. A linear increase in immune attack rate (α) with viral density (type 1 functional response) is assumed, such that the equation for viral growth is:

$$V'_w = \phi_{(t)}V - \alpha_{(t)}ZV_w.$$

While little is known about ATV innate immune evasion, larval salamanders are often referred to as immunodeficient and lack a proliferative lymphocyte response [33]. For example, we do know

from the axolotl model system that larval urodeles can mount innate immune responses to ATV, although this is not always very effective against the pathogen, leading to high susceptibility. We therefore model the immune system of the salamander host very generally.

We added demographic stochasticity to this model of within-host dynamics to account for random events that befall individuals and affect the interactions between the host's immune system and the virus. Importantly, this also allows us to account for the fact that some hosts clear infection, while others may sustain infection or die of infection. To add this source of stochasticity, we simulated the differential equations using a tau-leaping algorithm. Specifically, we simulate the within-host model (Z and V_w) 5 times per day by using a Poisson approximation. We also added daily variation in parameter values (ϕ, ψ, α) to account for environmental stochasticity, such that we have a mean and a standard deviation parameter for each value (e.g., ϕ_{mean} and ϕ_{sd}). This variation is incorporated by drawing the parameter from a Gaussian distribution each day using the given mean and variance. Furthermore, the parameters $\phi, \gamma, \psi, \alpha$, and $Z(0)$ are allowed to change over time as a function of temperature. As we will describe, we estimate a temperature-specific range for each of these parameters by fitting the model to our experimental data using a grid-search algorithm. This allows us to better understand how temperature might impact disease dynamics within the host.

4. Epizootic Model (Between-Host Model)

Our epizootic model links the processes that occur within the host, which determine the amount of virus shed into the water, to the transmission of the virus among host individuals, which determines the epizootic dynamics. We focus on the dynamics of ATV transmission within a single epizootic event, defined as an outbreak that occurs during a single larval salamander

developmental period. As described in Section 3, we begin with a classic SIR epidemiological model. Here, however, we have modified the system to include environmental virus and variation in host susceptibility (i.e., some hosts are more resistant, while others are more susceptible to becoming infected). With this model, we aim to simulate the spread of the virus between hosts under different temperature regimes. The epizootic dynamics are defined by:

$$S' = \frac{dS_{(t)}}{dt} = -\bar{\beta} S_{(t)} V_{(t)} \left(\frac{S_{(t)}}{S_{(0)}} \right)^{C^2}$$

$$V'_s = \frac{dV_{(t)}}{dt} = f(I_{(t)}) - \kappa V_{s(t)} .$$

Here susceptible hosts (S) at any given time point (t) may come in contact with the pathogen and become infected. The force of the infection is mediated by the concentration of virus that is shed into the water by the infected hosts (V_s). To account for variation in host susceptibility, we assume that there will be a decline in transmission over the course of the epizootic, as more susceptible individuals become infected first, leaving more resistant individuals later. Hosts that are either highly susceptible or resistant ultimately have a significant effect on the cumulative mortality during an ATV epizootic (Dwyer et al., 1997; Mihaljevic et al., 2019). We quantify this variation in susceptibility through the transmission rate by specifying an average transmission rate (i.e., susceptibility) in the host population ($\bar{\beta}$) and the coefficient of variation in transmission rate (C).

Once a susceptible individual becomes infected, we use the within-host model to explain how much of the virus is shed back into the environment by each infectious individual each day. Infectious hosts (I) then shed virus into the system at a rate that is dependent on the within host model (V_w) where the virus free-floating in the system will decay in the water column at a rate of

κ . As a result, we do not explicitly define the classes for I and R, which includes individuals that have died from infection or those who have cleared the infection, since they are both a function of the within-host model.

The model has several other important assumptions. The model assumes there is no host immigration and no host reproduction. Basically, the model assumes that adult salamanders laid eggs, those eggs hatched into larvae, and then the epizootic initiates among the available larvae in the wetland. Thus, transmission is only occurring within the larval population, and the epizootic ends with the conclusion of the larval development period. Furthermore, we assume that natural host mortality is negligible compared to the virus-induced mortality and we assume when a host dies of infection, they cease to contribute to shedding. Additionally, we assume transmission only occurs through contact with virions present in the water column and not through other mechanisms like cannibalism.

5. Fitting Within Host Model to Data

To estimate the key model parameters and how these parameters vary with temperature, we utilize maximum likelihood and a grid search method to fit the within-host model to the data collected in the laboratory experiment. Specifically, we fit the model to the time-series of cumulative mortality data (i.e., how many hosts have died from infection per day of the experiment). Since parameter magnitude can dramatically affect the dynamics of the model, we restricted each model parameter ($\phi, \delta, \psi, \alpha$) to a realistic positive, non-zero range defined by Mihaljevic et. al in 2019. However, since these parameter ranges were estimated for FV3 and only at ambient temperature, it is unclear how each parameter may be affected by temperature or

if the ideal parameter ranges for ATV are comparable. We therefore searched a broad range of possible parameters about these ranges to account for any uncertainties in unique viral biology.

We also estimated the initial immune component density ($Z(0)$) but the initial viral density in the host ($V_w(0)$) is held constant. Here, we assume it is possible that $Z(0)$ also varies across temperature treatments. For instance, the baseline immune functioning of the host could be better or worse, depending on the environmental temperature (Raffel et al., 2006; Rojas et al., 2005). While initial viral dose for each treatment is known, it is unclear how much virus in the water will enter the body and contribute towards $V_w(0)$ within each host. To account for this, we built stochasticity into the model that allows for some variation in $V_w(0)$ across individuals. We do not, however, estimate a unique $V_w(0)$ per dose of the experiment, because we do not have enough data to inform this estimation. Future work should clarify the relationship between initial dose in the water and dose that is absorbed into the host's body.

The grid search algorithm randomly and iteratively searches within each parameter range to discover high likelihood parameter sets. To calculate likelihoods, we compare the cumulative mortality each day from the experimental data to the cumulative mortality each day from the model for each given parameter set. Specifically, in the model, we simulate the within-host infection process for the same number of individuals that were exposed at each temperature in the experiment. Then, we determine how many of these individuals die on each day in the model, and we compare this to the experimental data using the following likelihood structure (L):

$$L_r = \sum_{i=1}^n \log(\text{Poisson}(D_i, M_i + 0.001)).$$

Here the cumulative mortality of the experimental data (D) for a given day (i) is compared to the same day in the model (M). Note that we add 0.001 to the model outcome to avoid an exact match between the model and the data for the value of zero, which can produce infinite values. We then log transform this probability density and sum across all days to get our final log-likelihood for each realization of the model (r) for a given set of parameters. Because the within-host model is stochastic, each time we run the model for a given number of individuals we expect randomness in how many individuals die each day. Therefore, we need obtain the mean likelihood (\bar{L}) across several model realizations to more accurately estimate a log-likelihood score for a given set of parameter values, as follows:

$$\bar{L}_j = \frac{\sum_{r=1}^R L_r}{R} .$$

Here, we take the average of the log-likelihoods across realizations of the model (R) for a given set of parameters(j). The grid search algorithm compares \bar{L} for each set of parameters as it searches through each parameter's range until we stop the grid search algorithm. At that time, the algorithm records the highest likelihood parameter set that was computed during that particular iteration.

To increase the efficiency of the grid search algorithm for high-likelihood parameter sets across a large parameter space, we used high performance computing and an “embarrassingly parallel” process. For a single grid search (performed on a single CPU) we looped through the parameters ten times, and we calculated likelihoods based on 30 stochastic model realizations. We repeated this process on 5000 CPUs using the Monsoon high-performance computing cluster at NAU. The resulting 5000 parameter sets were sorted by log-likelihood, and we kept the top 20% for each

temperature treatment. These sets were then used to simulate the within-host model, allowing us to quantify and visualize the fit of our model after accounting for parameter uncertainty.

6. Estimating Transmission Rates

To quantify the average and variation in susceptibility, we estimated the average transmission rate (i.e., susceptibility) in the host population ($\bar{\beta}$) and the coefficient of variation in transmission rate (C). Larger values of (C) mean that there is more variation among individuals in the host population. Importantly, our laboratory experiment allowed us to explicitly quantify these values and how they change along a thermal gradient, which we will describe below. These values of $\bar{\beta}$ and C then allow us to determine how many individuals become infected per time-step of the model (Dwyer et al., 1997; Mihaljevic et al., 2020).

We estimated parameters $\bar{\beta}$ and C and their relationship with temperatures by fitting the fraction of infected individuals at the end of the experiment to a modified epizootic model produced when solving the differential equation for S' :

$$-\log(1 - i_k) = \frac{1}{C_k^2} \log(1 + C_k^2 \bar{\beta}_k V_w(0) \hat{t})$$

This equation can be defined in terms of i , the fraction of infected individuals at the end of the experiment across each holding temperature (k) where we consider the initial dose treatment ($V_w(0)$), during the 3-day exposure period, \hat{t} . By fitting this equation to the experimental data, we can estimate the average transmission rate ($\bar{\beta}$) and variability in susceptibility in the host population (C) and determine how they vary across temperatures.

To understand how climate might influence disease dynamics between hosts in a population, we allow multiple parameters to be influenced by temperature. This allows us to utilize the model to simulate epizootics that occur in environments with fixed temperatures or in environments where temperature fluctuates over time. For $\bar{\beta}$, κ , and C , we assume a change over time as a function of temperature. Parameter ranges for decay rate across temperature treatments were estimated from studies focusing on the environmental drivers of FV3 (Munro et al., 2016), further studies of ATV viral decay rates are encouraged to better parameterize the effect of this parameter on this system.

7. Simulating the Full Model Under Climate Conditions

After we parameterized our within-host model and estimated transmission rates for each temperature, we could then use our full model, combining the within-host and between-host components, to simulate the effects of environmental temperature on virus epizootics in larval salamander populations. To explore temperature's effects on epizootics, we conducted simulations for two types of temperature regimes: a fixed temperature and a seasonal temperature scenario. Specifically, we fixed temperatures at either 15°C, 20°C, or 28°C, or temperatures followed a seasonal trend, shown in Figure 8. For the seasonal temperature trend, we simulated a scenario that reflects the current 'normal' and a hypothetical warming pattern, to explore possible effects of a warming climate. The normal temperature regime was based on the average water temperatures we measured across Arizona wetlands (Cooney & Mihaljevic, unpublished data). A warm temperature regime was characterized by introducing a warmer early season followed by a prolonged period of high temperatures followed by a period of cooling after the monsoon season and into fall (Kaushal et al., 2010). Note that these are rough

approximations of seasonality to explore the possible effects of temperature regimes on epizootic dynamics.

In addition, for each of these scenarios we varied the initial density of salamanders in the population. Since ranavirus transmission is density-dependent, we expect larger outbreaks in high density populations (Brunner et al., 2017). In nature, most larval salamander populations range from 50-500 hosts within 10,000L of water (Greer et al., 2008; van Buskirk & Smith, 1991). Therefore, we simulated epizootics at densities of 100 and 500 individuals per 10,000L of water. This will help to disentangle the effects of density and temperature on epizootic patterns. Under each of these scenarios, we introduced a single infectious individual into a population of larval salamanders to initiate the outbreak. We then simulated an epizootic over five months, consistent with the duration of the larval salamander growth period in Arizona (Greer et al., 2009). In these simulations, the model again included demographic stochasticity using a tau-leaping algorithm. We also incorporated parameter uncertainty. To do this, for each realization of the full model, we drew a random, high-likelihood parameter set for the within-host model.

RESULTS

1. Lab Experiment

Cumulative Mortality

Of the 228 individuals that were exposed to the virus, a total of 84 individuals died across all three temperature treatments. At the lowest temperature treatment, 15°C, 46% (38/82) of the infected individuals died whereas, 60% of the individuals died at 20°C (47/79), and only 13%

died at 28°C (9/67). Cumulative mortality peaked earlier and more rapidly at the intermediate temperature (20°C) than at the lowest and highest temperatures. At 15°C, while we observed some mortality as early as the 20°C treatment, we observed a significant delay (11 days) in the time at which cumulative mortality begins to increase rapidly. On the other hand, the time to

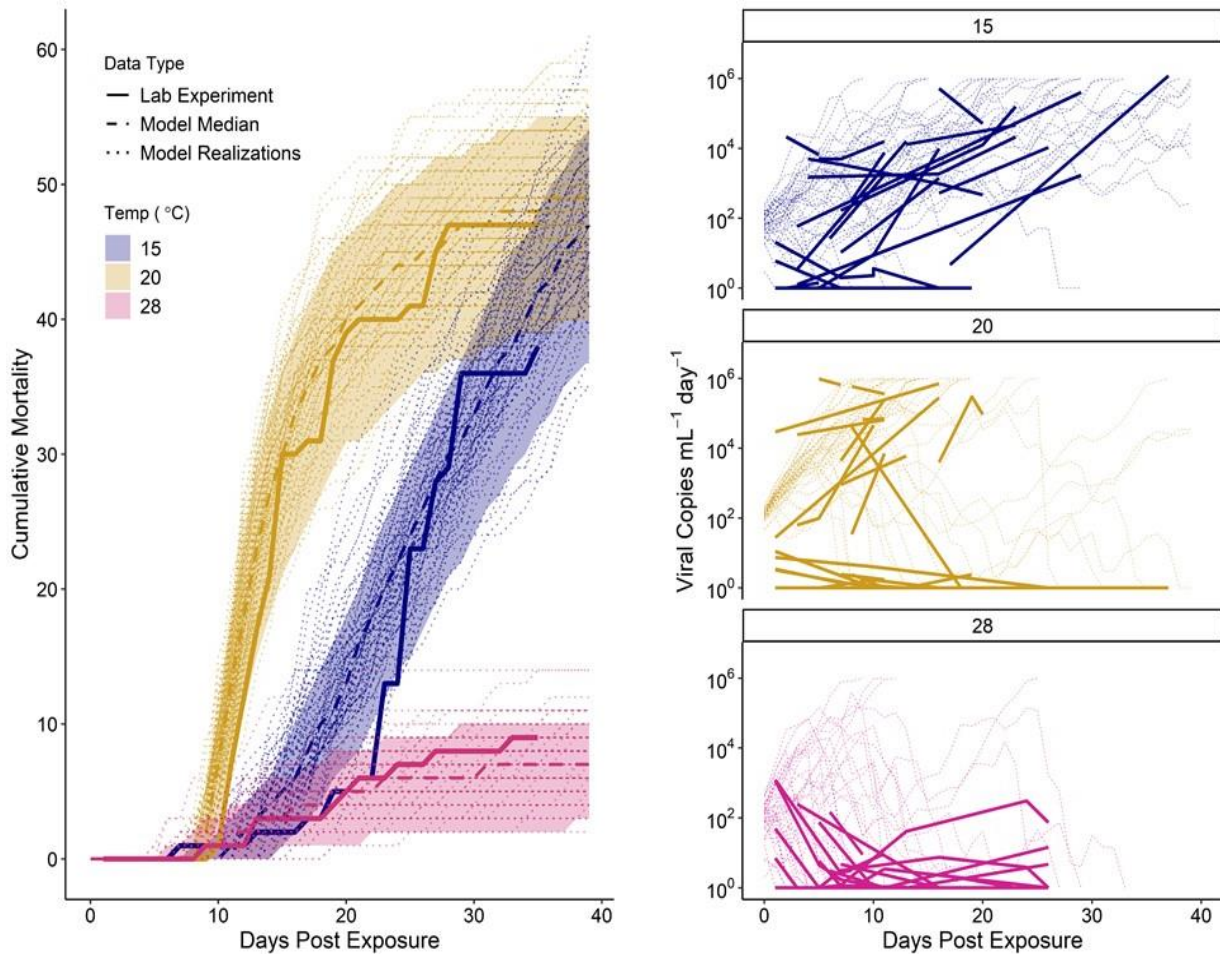


Figure 3: Model Fit to Data

Left: The cumulative mortality over time post exposure per temperature treatment (15°C = blue, 20°C = yellow, 28°C = purple) period during our experiment (solid line), our median model fit (dashed line), and the first 5 model realizations of the model (dotted line) using the parameter sets with the top 20 best log-likelihoods. The ribbon represents the 87.5% credible interval for our model. **Right:** The amount of virus shed into the environment (viral copies mL⁻¹day⁻¹) per individual across each temperature treatment for our laboratory experiment (solid lines) and our model (dotted lines). Shedding was estimated from a random subset of individuals during the experiment and from the first 5 model realizations of the model using the parameter sets with the top 20 best log-likelihoods.

mortality in the 28°C treatment was quite variable, with some individuals dying rapidly, but with some individuals dying very late in the experiment.

Shedding Rate

To quantify viral shedding rate, analyzed 328 randomly selected filters collected from 191 individuals at the different temperature and dose treatments. We noticed that at 20°C individuals had on average the highest shedding rates and the fastest increase in shedding rates over time (Fig 3 & 4). This was followed by the 15°C treatment, which had a slower rate of increase in

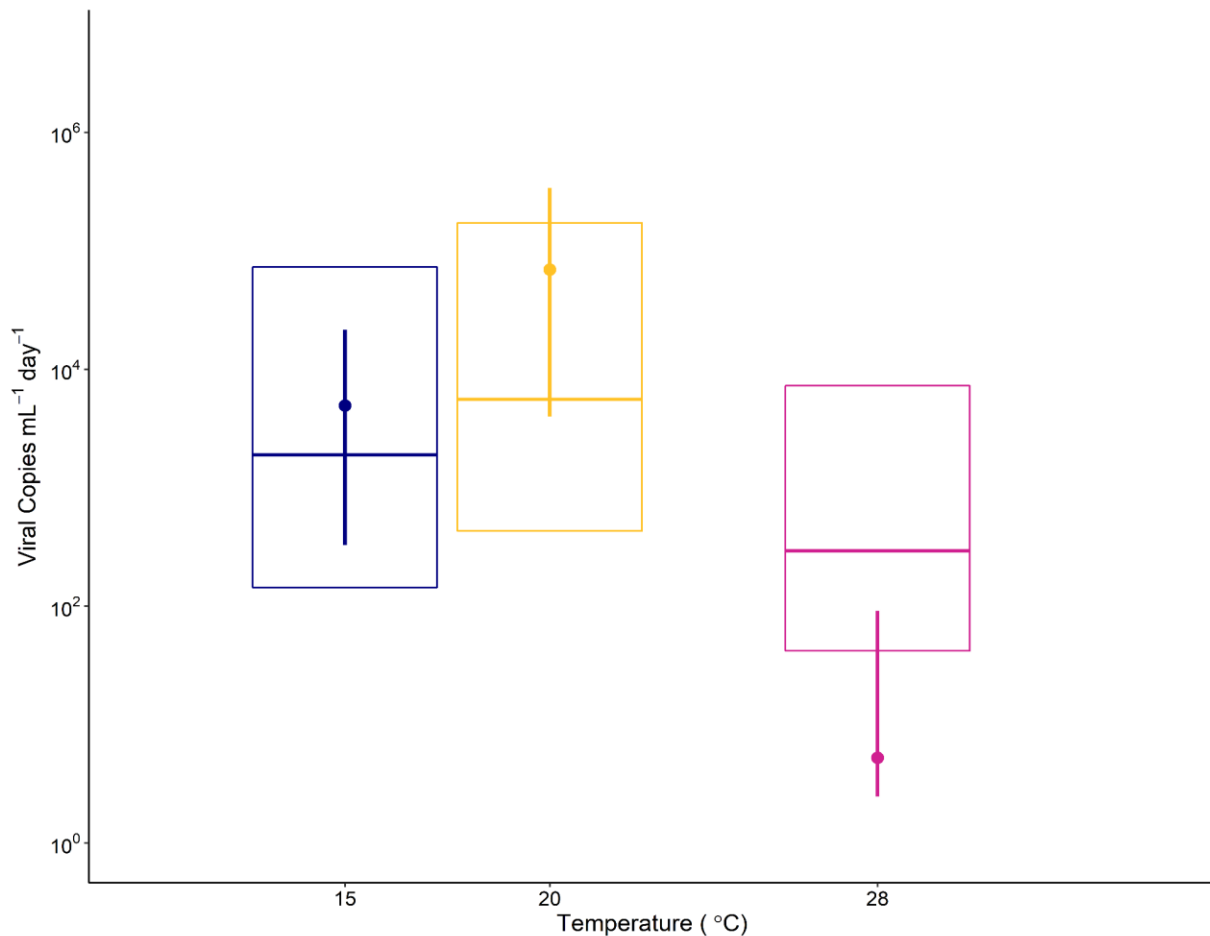


Figure 4: Average Shedding Rate

The average shedding rate (median and 87.5% credible intervals) was estimated from a random subset of individuals during the experiment (dot) and our model (box) across our three temperature treatments (15°C = blue, 20°C = yellow, and 28°C purple). Both the experiment and the model show virus is shed at a higher rate at intermediate temperatures (20°C) on average.

shedding over time, which led to a longer shedding period on average before mortality, which was also evidenced in our mortality data. At 28°C, which had the fewest infected individuals, there was on average very low shedding. No virus was detected in any control groups.

Interestingly, our experiment allowed us for the first time in this system to provide evidence that some larval salamanders clear ATV infection over time, or at least stop shedding the virus (e.g., quiescent virus (Grayfer et al., 2014, 2015; Samanta et al., 2021)). This corresponded with our model simulations, in which an individual may clear infection due to demographic stochasticity within the host. While there were anecdotal cases of virus clearance at all temperatures, we found this occur more frequently at 28°C (at least 8/15 individuals for which we had time series shedding data at 28°C, 3/16 for 20°C, and 3/20 for 15°C). For now, we ignore comparisons among viral doses because our within-host model ignores dose per se; however, we encourage future studies to expand upon our study with larger dose treatments, density, and a greater range of temperatures.

2. Fitting Within Host Model to Data

Cumulative Mortality

Our within-host model that describes the interactions between virus replication and immune system functioning explains the experimental data on mortality quite well (Fig 3). The model correctly explains the effects of temperature on cumulative mortality over time, such that 20°C yields the earliest and strongest peak in mortality, the coldest temperature results in a significant peak delay, and the highest temperature experiences low mortality. We only see a few deviations

of the model from the observed data, primarily early in the epizootic within the 15°C temperature treatment. At 15°C the model assumes that mortality starts ramping up a bit too early, which may be explained by our assumptions about viral dosage, described more later.

Our model shows that effects of temperature on mortality can be described by temperature-specific processes that occur within the host, captured by temperature-specific parameter values. The only parameters to increase with temperature are immune attack rate (α) and immune component growth in response to the virus (ψ), where the median parameter values for 28°C are significantly higher than those for 15 and 20°C. Interestingly, the model also reveals that there is a non-linear relationship between temperature and the parameter values for half saturation constant (γ), viral replication rate (ϕ), rate of natural immune component decline (δ), and

Table 1: Parameter Estimates

Parameter estimates (median and 95% credible intervals) across each of our temperature treatments from our within-host model.

Parameter	Description	Units	15°C	20°C	28°C
$V_w(0)$	Initial Viral Density	Viral DNA copy (VC)		50	
$Z(0)$	Initial immune component density	Immune component (IC)	3.089(0.343-6.072)	0.934(0.024-3.975)	1.32(0.029-5.363)
δ	Rate of immune component decline to homeostasis	day ⁻¹	3.116(0.777-4.89)	2.814(0.628-4.443)	3.803(0.843-5.477)
N_z	Immune component constant rate of production	(IC)day ⁻¹		$\delta_k Z(0)_k$	
γ	Half saturation constant	Viral DNA copy (VC)	0.732(0.074-1.275)	0.513(0.078-1.112)	0.721(0.083-1.179)
ϕ mean	Average viral replication rate	day ⁻¹	4.86(1.702-11.566)	4.13(1.352-5.461)	4.791(1.75-5.853)
ϕ std dev	ϕ Standard Deviation	day ⁻¹	0.649(0.083-1.349)	0.821(0.055-1.081)	0.961(0.074-1.129)
α mean	Average mass-action attack rate	(IC) ⁻¹ day ⁻¹	0.916(0.271-12.289)	1.013(0.292-6.359)	5.406(0.608-7.039)
α std dev	α Standard Deviation	(IC) ⁻¹ day ⁻¹	0.729(0.074-1.173)	0.916(0.128-1.182)	0.876(0.22-1.105)
ψ mean	Average rate of immune component growth in response to virus	day ⁻¹	0.843(0.167-4.304)	0.812(0.24-3.997)	3.217(0.17-4.268)
ψ std dev	ψ Standard Deviation	day ⁻¹	0.292(0.061-0.612)	0.457(0.057-0.529)	0.463(0.078-0.571)

initial density of immune components ($Z(0)$). The 20°C temperature treatment had the lowest parameter values compared across all temperatures. In other words, the model predicts that at intermediate temperatures (20°C), both viral replication and the host's immune system must have lower rates to explain the mortality data. When temperatures are low (15°C), the initial density of immune components is high, but immune response is slower, and viral replication is moderate which explains the delayed peak in mortality. However, at 28°C the host's immune response to

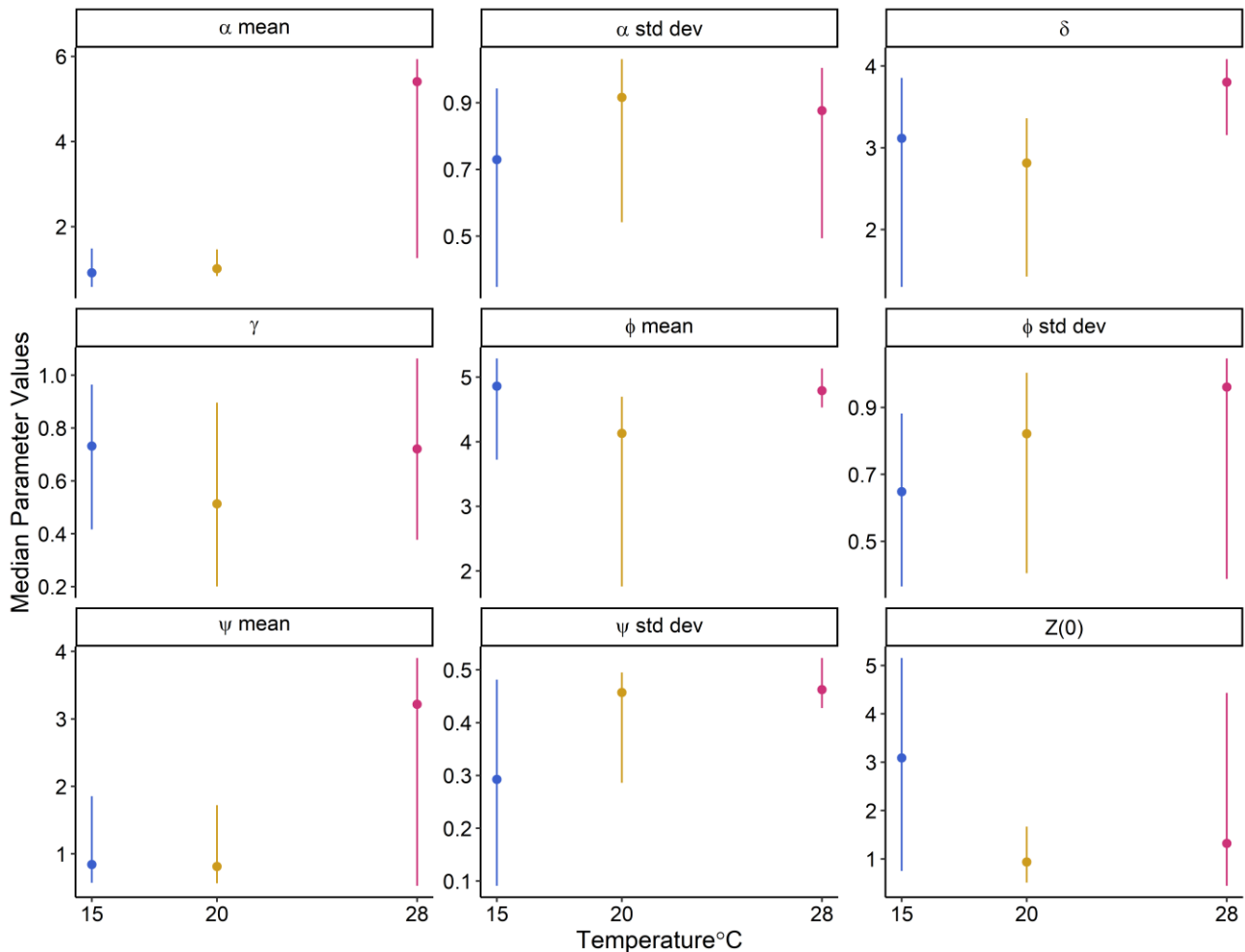


Figure 5: Parameter Estimates

Visual representation of our parameter estimates (median and 50% credible intervals) across each of our temperature treatments from our within-host model, emphasizing the non-linear relationships between some parameters (such as γ) and temperature.

the virus is most optimal and high immune functioning lead to lower mortality and higher clearance.

Shedding Rate

We further validated our model fit by checking if the parameterized model matched well to the observed patterns in virus shedding. While we did not fit the model to these data, the model does a good job of describing the amount of virus shed from each individual across temperature treatments. Here, the model correctly predicts the highest rate of clearance, and the lowest amount of shedding should occur at 28°C, low clearance, and high rate of shedding at 20°C, followed by prolonged periods of shedding and low clearance at 15°C (Fig 3 & 4). Furthermore, we can calculate the average shedding rate for each temperature treatment and compare the results of the fitted model to the experimental results. Our model is consistent with our experimental data such that, on average, the virus is shed at a higher rate at 20°C (Fig 4).

3. Estimating Transmission Rates

Utilizing the expression $-\log(1 - i_k)$, derived from our epizootic model, we were able to evaluate the effects of temperature on the variation in host susceptibility. To quantify this variation in host susceptibility, we estimated the average transmission rate ($\bar{\beta}$) and the variability in susceptibility in the host population (C). We observed relatively consistent average transmission rates across temperature treatments (15°C: 3.6, 20°C:3.0, 28°C: 5.5 day⁻¹virus⁻¹uL⁻¹), suggesting that the average susceptibility is not significantly affected by temperature (Fig 6). However, when evaluating the impact of temperature on C , we observe significantly higher variation at 28°C (Fig 6). This suggests that we see a significantly higher variation in host

susceptibility to infection at higher temperatures. Here we do not see a difference in the variability in susceptibility at 20°C and 15°C (Fig 6). The fraction of infected, i , was estimated using the presence or absence of viral symptoms and mortality events, due to issues processing the tissue samples. This implies that the model may underestimate the average transmission rate if there were asymptomatic individuals. However, prior literature shows that asymptomatic disease is quite rare (Brunner et al., 2005).

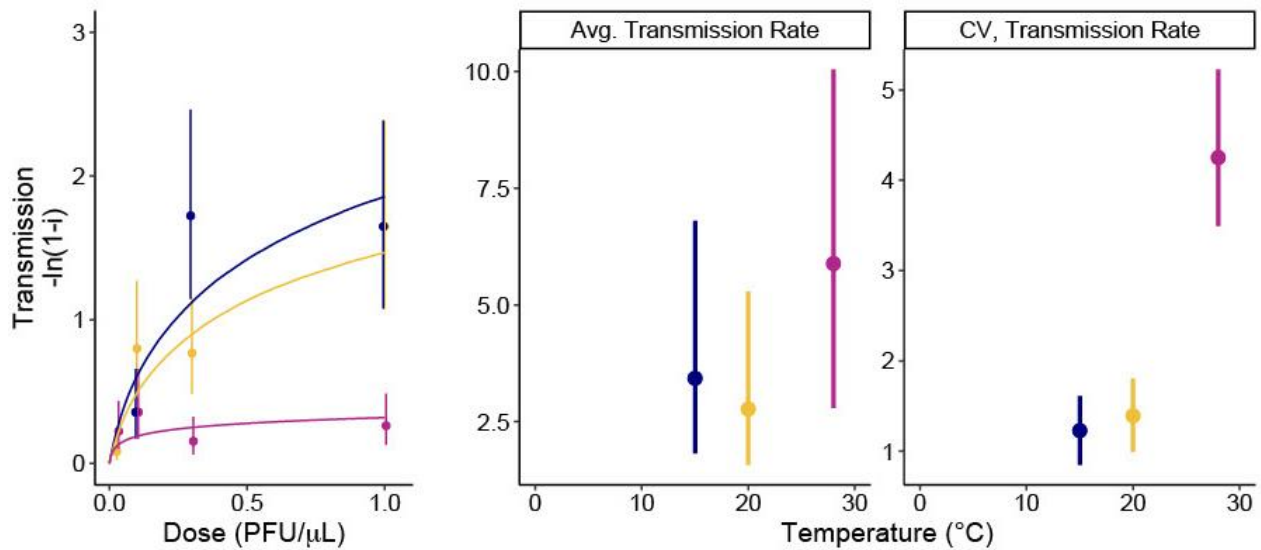


Figure 6: Estimating Transmission Rate

From the experimental data, we were able to estimate the average transmission rate and coefficient of variation in transmission rate (CV) at each temperature (15°C = blue, 20°C = yellow, and 28°C purple). We used the expression $-\ln(1-i)$ which is equivalent to $-\log(1-i_k)$, which is derived from our epizootic model, where we define i as the fraction of infected hosts at the end of the experiment for each temperature-dose treatment. Here we plot the median average transmission rate and CV and the 95% credible intervals for each temperature.

4. Simulating the Full Model Under Climate Conditions

Fixed Temperatures

When we simulated epizootics at constant (fixed) temperatures, we observed earlier and more rapid outbreaks at 20°C, which peaked about 25 days after initiation. At 15°C, we see a delayed peak around 50 days which is nearly a month later compared to 20°C. The rate of infection at 15°C also appears to be slower with a more gradual ramp-up period. While the epidemic at 20°C produced an earlier peak, the total proportion infected over the outbreak is similar to that of the 15°C treatment. Furthermore, the cumulative fraction of infected individuals (i.e., the total epizootic size) is lower at 15°C compared to 20°C. At 28°C, while we see a peak in the fraction of infected individuals around 35 days, we also see a dramatically smaller epizootic size. Interestingly, we also see a large degree of variability in epizootic dynamics at 15°C and 28°C compared to 20°C.

Effects of Density

Unexpectedly, for each temperature the difference in the cumulative fraction of infected individuals between the high (500 individuals per 10,000L water) and low (100 individuals per 10,000L water) was negligible (Fig 7). However, at high densities, we see less variable epizootic dynamics, which leads to a higher average cumulative fraction infected for each temperature.

Fluctuating Temperature Regimes

When using the full model to simulate a fluctuating temperature regime over a full season under normal and warmed temperature scenarios, we see a distinct difference in the size and timing of the outbreaks. When considering a scenario where temperatures are warmer in the early season, we observed earlier (~15-20 days) and higher peaks in the fraction of infected individuals. At the

beginning of the epidemic, we also see less cumulative infections and a more rapid outbreak under this warmed climate regime than observed under a season with a typical climate regime. However, later in the season, we see a small second peak in the fraction of infectious individuals develop under the warmed scenario. While ideal intermediate temperatures (20°C) early in the season lead to stronger outbreak early on, an earlier and prolonged exposure to high temperatures (28°C) cause a decrease in transmission and the outbreak consequently declines (i.e., starts to burn out) earlier and more rapidly. This leaves leftover susceptible individuals vulnerable to infection as temperatures begin to decline again into the optimal temperature window, leading to a second, but smaller epizootic late in the season. It is also interesting to note that we observed more variable dynamics in the ‘normal’ temperature regime.

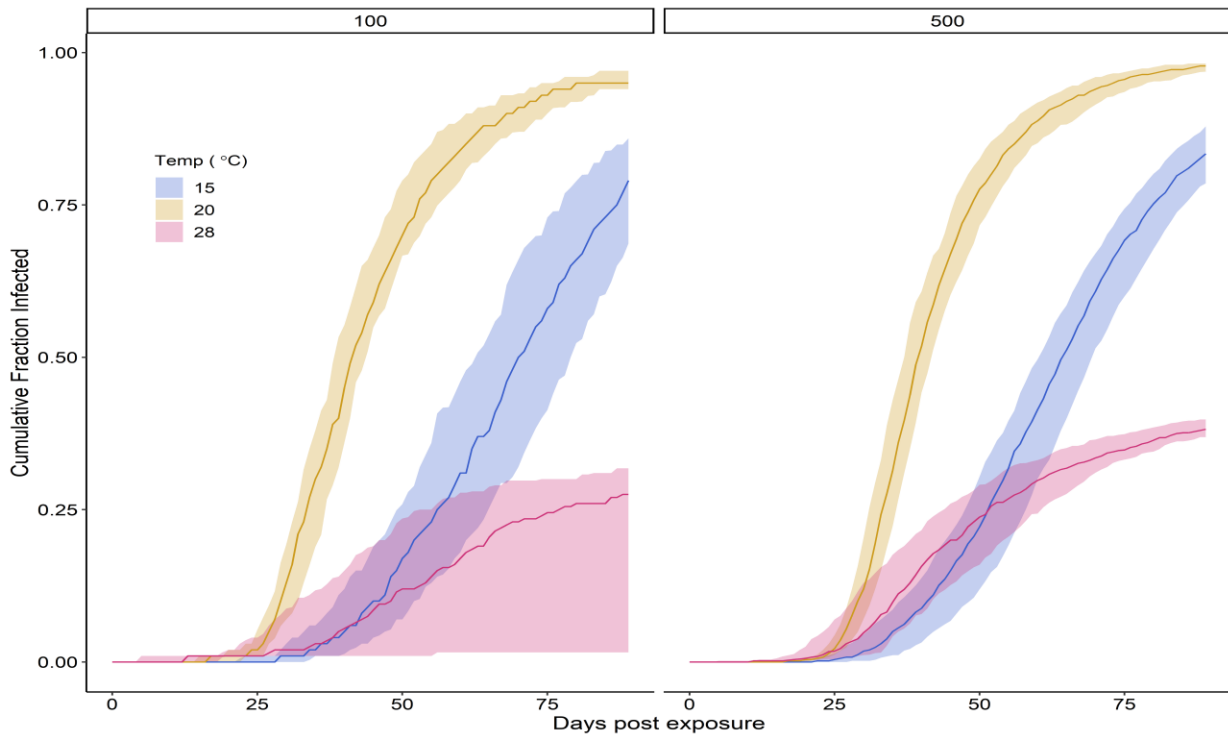
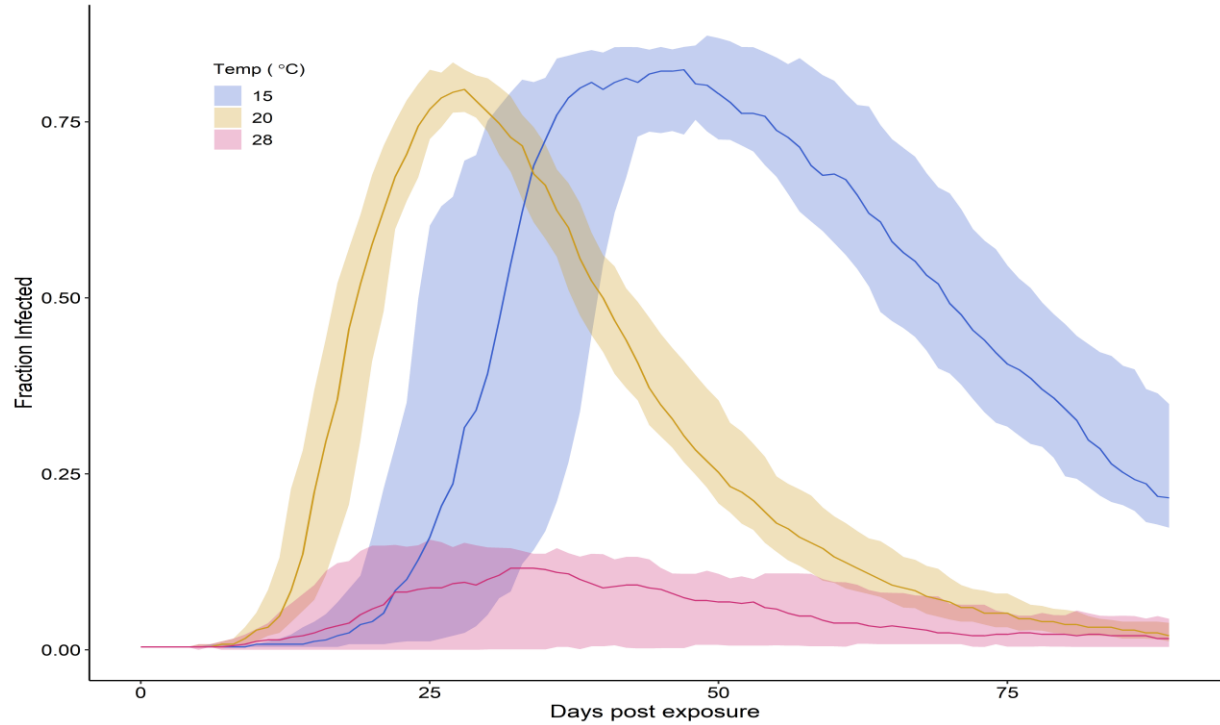


Figure 7: Effects of Fixed Temperatures and Density on Epizootics

Top: The effects of fixed temperatures (15°C = blue, 20°C = Yellow, and 28°C = purple) on epizootics simulated by our full epizootic model. Here we focus on the effects of temperature on the fraction of infected individuals. **Bottom:** We take these simulations a step further by considering the effects of both density and fixed temperatures on an epidemic, where we focus on the cumulative fraction infected over time.

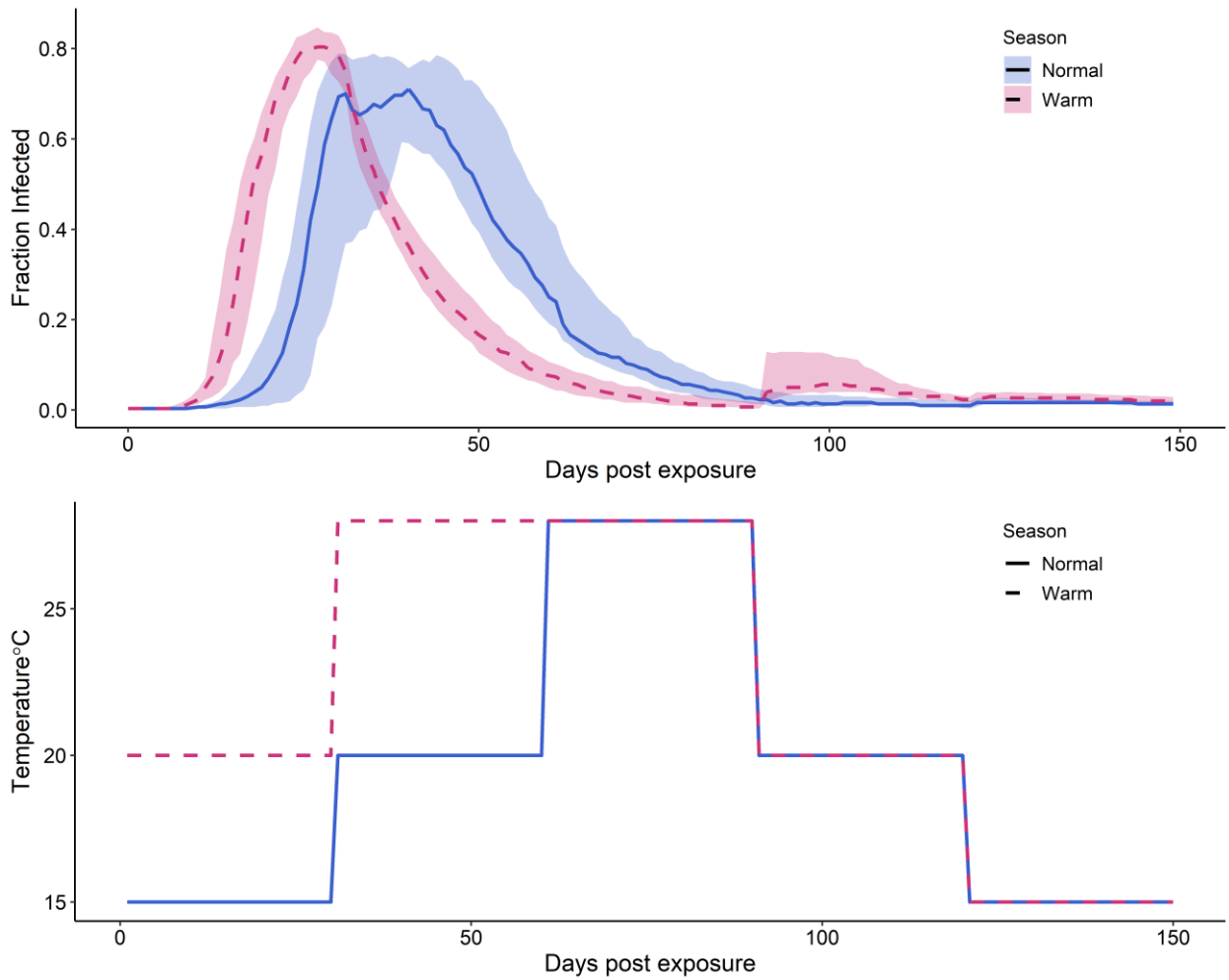


Figure 8: Simulating Fluctuating Temperatures Regimes

Top: The fraction of infected over time under ‘normal’ temperature regimes (dashed purple), defined by average seasonal temperatures across Arizona, and a ‘warm’ temperature regime (solid blue), characterized by a warmer early season. Bottom: Each seasonal temperature regime lotted over time.

DISCUSSION

This research indicates that water temperature during the developmental period of larval salamanders may play a significant role in the emergence, timing, and size of ATV outbreaks in *A. mavortium* populations. Here, we might expect increasing temperatures to lead to higher replication and mortality rates in highly infectious ranavirus species such as ATV (Brand et al., 2016; Chinchar, 2002). Other salamander based-ATV infection studies also suggest intermediate temperatures are optimal for ATV infection and pathogenesis (Rojas et al., 2005). However, amphibian immune systems temperature may fluctuate wildly with seasonal temperature changes impacting host response to infection, such that decreased temperatures lead to a reduction in immune response in amphibian hosts (Brand et al., 2016; J. K. Jancovich & Jacobs, 2011; Lips et al., 2008; Raffel et al., 2006). As a result, amphibian-pathogen systems are expected to have a strong relationship with temperature where there are complex trade-offs between viral replication and immune. In this study we show cumulative mortality and shedding rate peak at intermediate (20°C) temperatures. Therefore, our results generally support this idea by revealing a clear non-linear relationship between temperature and both mortality and shedding rates that is mediated by pathogen replication and host immune response.

At low temperatures (15°C), our data suggest hosts possess a high initial population of immune cells which may be able to compete with viral replication for a period of time. However, as immune components are removed from the system, they are replaced slowly at low temperatures which may give the pathogen an opportunity to eventually outcompete the impaired host immune response. Studies show that as temperatures decrease, both the dissemination of the virus to distal organs, apoptosis of infected cells, and antimicrobial peptide activity also decrease (Brand

et al., 2016; Chen & Robert, 2011; Chinchar et al., 2001). Our study shows that at temperatures (20°C), the initial population of immune components is low, immune response is low, and viral replication is low. This suggests that although viral replication is low, it does not have to compete with a high initial density of immune cells, allowing viral replication to increase with little competition causing an earlier and more rapid peak in mortality. Therefore, enhanced ATV caused mortality at intermediate temperatures and lower temperatures suggests immune components may be inhibited (Rojas et al., 2005).

Interestingly, we find a deviation from the experimental data and the predicted within-host model for the 15°C treatments, particularly at the early stages of an infection. We believe this deviation is a direct result of not considering dose as a model parameter. In the future, this could easily be incorporated into the model by increasing the amount of data at each dose treatment. This would enable the effects of dose on delayed mortality to be studied further. Our work shows tentative evidence that the delay seen at lower temperatures may increase with lower doses, causing a discrepancy between the best-fit model and the data during this critical transitional period.

The highest temperature, 28°C, on the other hand, appears to have a moderate initial density of immune cells, a strong immune response, and a moderate viral replication. While viral replication is moderate at 28°C, there is far more competition with the immune system. Unlike the 15°C treatment, at 28°C there is a slightly weaker starting immune system which could explain some of the rapid deaths observed at the beginning of the epizootic. Here the immune system at colder temperatures is generally able to outcompete viral replication once those initial immune cells have been depleted. Whereas, at 28°C, the immune response can rapidly respond

and is more easily able to outcompete the virus. Therefore, ATV the peak in epizootics in the field during spring and fall may be related to these interactions between temperature, immune response, and viral replication (Greer et al., 2009).

While temperature does not appear to significantly impact the average transmission rate in this study, the variation in host susceptibility increases with temperature. We not only observed fewer hosts become infected and more hosts clear the infection at 28°C temperature treatments, but we also observed individuals who became infected at low doses or died quickly from infection. This suggests at higher temperatures (28°C) we see a higher variation in a host's resistance to ATV infection, such that increased temperature may be a double-edged sword for salamander hosts, good for some individuals and bad for others. The increased variation in host susceptibility at high temperatures (28°C) could be explained by variation in immune response attributed to increased physical stress (Brand et al., 2016) and improved phagocyte performance (Brand et al., 2016; J. K. Jancovich & Jacobs, 2011; Raffel et al., 2006) at high temperatures.

However, relatively little is known about the interaction between the innate immune system of larval salamanders and ATV (J. K. Jancovich & Jacobs, 2011). At intermediate temperatures, larval African clawed frog, *Xenopus laevis* have innate immune systems that initiate robust responses to FV3 infection within one week of infection (Grayfer et al., 2014, 2015). These studies show that larval amphibians such as *X. laevis* have interferon (IFN)-like responses to FV3 (Grayfer et al., 2014, 2015), however, no IFN-like molecules have been directly identified in larval salamanders (J. K. Jancovich & Jacobs, 2011). Despite this, some studies based on antiviral responses propose larval salamanders have an interferon (IFN)- and protein kinase R

(PKR)-like enzyme based immune system (J. K. Jancovich & Jacobs, 2011). Here, infection stimulates a response from these innate immune components which interfere with the cellular replication of infected cells and consequently, the virus. Unlike FV3, studies show that ATV may employ proteins to evade the host innate immune system. These enzymes may directly interfere with the IFN-inducible PKR, causing degradation of the anti-viral enzyme and enhancing pathogenesis (Chen & Robert, 2011; J. K. Jancovich & Jacobs, 2011). Therefore, we encourage further research and alternative model testing to fully understand if our model fully encompasses the interaction between the immune system and pathogen.

The exposure of a non-local ATV strain to larval salamanders in the experiment could also be a potential source of the observed variation in susceptibility. While all the populations from which we collected salamander egg masses are all relatively equidistant from the location where we isolated ATV, it is possible some populations may show an increase or decrease in susceptibility to infection when exposed to different ATV strains. Studies have shown that mortality rates significantly vary among salamander populations with similar ecology when exposed to different ATV strains and the origin of the salamander may impact how virulence differs across strains (Schock et al. 2009). Here they hypothesized that local selection pressures may have a significant effect on this widespread and diverse host-pathogen system, which may ultimately lead to variation in susceptibility both locally and across regions (Schock et al. 2009). However, little is known about what factors might influence a population's susceptibility to different ATV strains. Studies in other ranavirus systems have described differences in pathology across strains of the same ranavirus species (Cunningham et al. 2007) and differences in genetic diversity across host populations may also contribute to variation in epizootics (Prearman & Garner 2005). While we

sought to avoid an effect of population on our study by selecting sites within the same region and randomly assigning individuals to different treatment groups, further analyses are needed to assess if we did observe different responses to ATV across different populations in this study. Nonetheless, future studies are needed to further evaluate the effects of phenotypic and genetic variation within host populations and ATV strains on disease dynamics.

Like previous trends in our study, when we simulate the effects of fixed temperature regimes on epizootics during the developmental season of larval salamanders, we see earlier and more rapid outbreaks at when temperatures are 20°C (Fig 7). Interestingly, while we see a delayed peak in the proportion of infected individuals at 15°C, we see a similar cumulative number of infected individuals. This may be partially explained by the observed spread of the peaks in the fraction of infectious individuals. At low temperatures (15°C), the peak in proportion of infected individuals is nearly double the spread of the peak at 20°C. Intermediate temperatures (20°C) seem to not only produce earlier and more rapid outbreaks, but outbreaks that persist over a shorter time period. Epizootics at cooler temperatures (15°C), on the other hand, seem to produce a prolonged period of infection and consequently result in a significantly longer outbreak that eventually results in similar final proportion of infected individuals at the end of the season. Other studies have shown that at colder temperatures, the time to death may decrease but viral load increases (Rojas et al., 2005). We hypothesize that individuals at 15°C shed for longer periods of time, which may maintain higher levels of virus in the water column for longer time periods in order to infect susceptible individuals over longer periods of time. As a result, an epizootic event may take longer to ramp-up by will, over time, become equally as large.

When considering the effects of fixed temperatures with epizootic simulations over fluctuating temperature regimes, we can begin to understand how climate change may affect ATV epizootics. During a 'normal' season, characterized by the average seasonal water temperatures observed in Arizona (Cooney & Mihaljevic, unpublished data), we see an infectious period spanning nearly two months (Fig 8). When considering a climate change regime reflecting warmer early season conditions, we see an epidemic that is not only earlier in the season but more rapid. However, this rapid epizootic event allows for a higher rate of survival in the early season due to plummeting transmission during the warmest periods of the season. As temperatures decline, the remaining susceptible individuals become vulnerable to infection again which results in a second much smaller outbreak at the end of the season. This poses a concerning possibility, the emergence of a bimodal pattern of transmission.

As the climate warms, it is hypothesized that we may begin to see a shift from one to two peaks in transmission where a pathogen's optimum thermal range now occurs both early and late in the season (Altizer et al., 2013). A long-term reduction in variability in resistance to disease with temperature can also cause a significant shift in disease dynamics, where outbreak cycles may become increasingly unstable. In turn, the loss of highly resistant individuals in host populations may lead to large outbreak events, particularly in populations with high host densities (Brand et al., 2016; Dowell, 2001; Dwyer et al., 1997). Surprisingly, we did not see an effect of density on ATV disease dynamics despite being well documented for ranaviruses (Dwyer et al., 1997). However, it is likely that density does not have a linear effect on dynamics, such that we may only see an effect between more extreme differences in density than we tested in this study.

A bimodal or unstable pattern of transmission might subsequently increase a pathogen's temporal range which may cause the pathogen to encounter a greater range of susceptible hosts and populations. It is hypothesized that chronically infected larvae and adults may not only be a major contributor towards the spread of the pathogen but also outbreak initiation. Warming temperatures have led to increased host ranges and the subsequent increased distribution of tick-borne diseases naive populations (McPherson et al., 2017). Since ATV cannot be not vertically transmitted, it is unknown how recurrent ATV epizootics are initiated in wetlands (Dwyer et al., 1997). It is possible that overwintering larvae or branchiate adults may serve as reservoirs for the virus to over-winter. Historical sites near the North Rim of the Grand Canyon in Northern Arizona have experienced seasonal epizootics since the 1980's, despite completely freezing each season preventing the establishment of overwintering larvae or branchiate adults. Alternatively, chronically infected adults could shed virions into the wetland during breeding subsequently exposing the future larvae, however, there is little evidence to support this claim (Dwyer et al., 1997). Preliminary field results also suggest that ATV may be infecting other non-salamander amphibian and reptile species such as federally threatened frog (*Rana chiricahuensis*) and snake species (*Thamnophis rufipunctatus*). Therefore, two peaks in transmission could allow a greater number of chronically infected hosts to spread the virus to other populations and for an increased chance of infecting naive hosts that would not encounter the pathogen otherwise. Therefore, we recommend future research focuses on collecting time-series field and laboratory data from sites that vary over a diverse thermal range in order to fit the epizootic model to more realistic set of temperature ranges and population densities.

Both human diseases (e.g., influenza, measles, rotavirus) and wildlife diseases (i.e., snake fungal disease, white-nose fungus) have recurrent seasonal disease outbreaks where temperature heavily influences the shape of the epizootic (Altizer et al., 2006, 2013; Hudson et al., 2002). For example, temperature-induced tradeoffs between parasite development, transmission, and mortality have a strong impact on infection patterns. Here we a warming trend may lead to a shift from one to two peaks in transmission can be observed and predicted (Altizer et al., 2006; Molnár et al., 2013). Models such as ours could be important for better understanding the effects of climate change on disease dynamics, where projections could aid in developing intervention protocols and conservation efforts to help reduce or prevent outbreaks. In conclusion, our model, while limited, could also be adapted for several systems in which the host sheds infectious pathogenic particles into the environment. Our study improves upon both the current knowledge of ATV disease dynamics and model-based methods of understanding the effects of climate change on disease.

REFERENCES

- Allender, M. C., Mitchell, M. A., Torres, T., Sekowska, J., & Driskell, E. A. (2013). Pathogenicity of Frog Virus 3-like Virus in Red-eared Slider Turtles (*Trachemys scripta elegans*) at Two Environmental Temperatures. *Journal of Comparative Pathology*, *149*(2–3), 356–367. <https://doi.org/10.1016/j.jcpa.2013.01.007>
- Altizer, S., Dobson, A., Hosseini, P., Hudson, P., Pascual, M., & Rohani, P. (2006). Seasonality and the dynamics of infectious diseases. *Ecology Letters*, *9*(4). <https://doi.org/10.1111/j.1461-0248.2005.00879.x>
- Altizer, S., Ostfeld, R. S., Johnson, P. T. J., Kutz, S., & Harvell, C. D. (2013). Climate Change and Infectious Diseases: From Evidence to a Predictive Framework. *Science*, *341*(6145), 514–519. <https://doi.org/10.1126/science.1239401>
- Ariel, E., Nicolajsen, N., Christophersen, M.-B., Holopainen, R., Tapiovaara, H., & Bang Jensen, B. (2009). Propagation and isolation of ranaviruses in cell culture. *Aquaculture*, *294*(3–4). <https://doi.org/10.1016/j.aquaculture.2009.05.019>
- Brand, M. D., Hill, R. D., Brenes, R., Chaney, J. C., Wilkes, R. P., Grayfer, L., Miller, D. L., & Gray, M. J. (2016). Water Temperature Affects Susceptibility to Ranavirus. *EcoHealth*, *13*(2). <https://doi.org/10.1007/s10393-016-1120-1>
- Brunner, J. L., Beaty, L., Guitard, A., & Russell, D. (2017). Heterogeneities in the infection process drive ranavirus transmission. *Ecology*, *98*(2), 576–582. <https://doi.org/10.1002/ecy.1644>
- Brunner, J. L., Richards, K., & Collins, J. P. (2005). Dose and host characteristics influence virulence of ranavirus infections. *Oecologia*, *144*(3). <https://doi.org/10.1007/s00442-005-0093-5>
- Brunner, J. L., & Yarber, C. M. (2018). *Evaluating the Importance of Environmental Persistence for Ranavirus Transmission and Epidemiology* (pp. 129–148). <https://doi.org/10.1016/bs.aivir.2018.02.005>
- Chen, G., & Robert, J. (2011). Antiviral immunity in amphibians. *Viruses*, *3*(11). <https://doi.org/10.3390/v3112065>
- Chinchar, V. G. (2002). Ranaviruses (family Iridoviridae): emerging cold-blooded killers. *Archives of Virology*, *147*(3). <https://doi.org/10.1007/s007050200000>
- Chinchar, V. G., Wang, J., Murti, G., Carey, C., & Rollins-Smith, L. (2001). Inactivation of Frog Virus 3 and Channel Catfish Virus by Esculentin-2P and Ranatuerin-2P, Two Antimicrobial Peptides Isolated from Frog Skin. *Virology*, *288*(2), 351–357. <https://doi.org/10.1006/viro.2001.1080>

- Collins, J., Jones, T. R., & Berna, H. J. (1988). Conserving genetically distinctive populations: the case of the Huachuca tiger salamander (*Ambystoma tigrinum stebbinsi* Lowe). *General Technical Report - US Department of Agriculture, Forest Service, RM-166*, 45–53.
- Collins, J. P., & Snyder, J. (2002). Sonora Tiger Salamander (*Ambystoma Tigrinum Stebbinsi*) New Mexico Draft Recovery Plan 2018. *Technical Report, Arizona Game And Fish Department, Nongame And Endangered Wildlife Program Technical Report* .
- Cunningham, A. A., Hyatt, A. D., Russell, P., & Bennett, P. M. (2007). Emerging epidemic diseases of frogs in Britain are dependent on the source of ranavirus agent and the route of exposure. *Epidemiology and Infection*, *135*(7), 1200–1212.
<https://doi.org/10.1017/S0950268806007679>
- Dowell, S. F. (2001). Seasonal variation in host susceptibility and cycles of certain infectious diseases. *Emerging Infectious Diseases*, *7*(3). <https://doi.org/10.3201/eid0703.010301>
- Duffus, A. L. J., Waltzek, T. B., Stöhr, A. C., Allender, M. C., Gotesman, M., Whittington, R. J., Hick, P., Hines, M. K., & Marschang, R. E. (2015). Distribution and Host Range of Ranaviruses. In *Ranaviruses* (pp. 9–57). Springer International Publishing.
https://doi.org/10.1007/978-3-319-13755-1_2
- Dwyer, G., Elkinton, J. S., & Buonaccorsi, J. P. (1997). Host heterogeneity in susceptibility and disease dynamics: tests of a mathematical model. *The American Naturalist*, *150*(6).
<https://doi.org/10.1086/286089>
- Epstein, B., & Storfer, A. (2015). Comparative Genomics of an Emerging Amphibian Virus. *G3 (Bethesda, Md.)*, *6*(1). <https://doi.org/10.1534/g3.115.023762>
- Grassly, N. C., & Fraser, C. (2006). Seasonal infectious disease epidemiology. *Proceedings of the Royal Society B: Biological Sciences*, *273*(1600).
<https://doi.org/10.1098/rspb.2006.3604>
- Gray, M. J., & Chinchar, V. G. (Eds.). (2015). *Ranaviruses: Lethal Pathogens of Ectothermic Vertebrates*. Springer International Publishing. <https://doi.org/10.1007/978-3-319-13755-1>
- Grayfer, L., de Jesus Andino, F., & Robert, J. (2014). The Amphibian (*Xenopus laevis*) Type I Interferon Response to Frog Virus 3: New Insight into Ranavirus Pathogenicity. *Journal of Virology*, *88*(10), 5766–5777. <https://doi.org/10.1128/JVI.00223-14>
- Grayfer, L., de Jesús Andino, F., & Robert, J. (2015). Prominent Amphibian (*Xenopus laevis*) Tadpole Type III Interferon Response to the Frog Virus 3 Ranavirus. *Journal of Virology*, *89*(9), 5072–5082. <https://doi.org/10.1128/JVI.00051-15>
- Greer, A. L., Briggs, C. J., & Collins, J. P. (2008). Testing a key assumption of host-pathogen theory: density and disease transmission. *Oikos*, *117*(11). <https://doi.org/10.1111/j.1600-0706.2008.16783.x>

- Greer, A. L., Brunner, J. L., & Collins, J. P. (2009). Spatial and temporal patterns of Ambystoma tigrinum virus (ATV) prevalence in tiger salamanders *Ambystoma tigrinum nebulosum*. *Diseases of Aquatic Organisms*, 85(1). <https://doi.org/10.3354/dao02061>
- Hall, E. M., Goldberg, C. S., Brunner, J. L., & Crespi, E. J. (2018). Seasonal dynamics and potential drivers of ranavirus epidemics in wood frog populations. *Oecologia*, 188(4). <https://doi.org/10.1007/s00442-018-4274-4>
- Hoverman, J. T., Mihaljevic, J. R., Richgels, K. L. D., Kerby, J. L., & Johnson, P. T. J. (2012). Widespread co-occurrence of virulent pathogens within California amphibian communities. *EcoHealth*, 9(3). <https://doi.org/10.1007/s10393-012-0778-2>
- Hudson, P. J., Rizzoli, A., Grenfell, B. T., Heesterbeek, H., & Dobson, A. P. (2002). *The Ecology of Wildlife Diseases*. Oxford University Press.
- Jancovich, J., Davidson, E., Morado, J., Jacobs, B., & Collins, J. (1997). Isolation of a lethal virus from the endangered tiger salamander *Ambystoma tigrinum stebbinsi*. *Diseases of Aquatic Organisms*, 31. <https://doi.org/10.3354/dao031161>
- Jancovich, J. K., & Jacobs, B. L. (2011). Innate immune evasion mediated by the *Ambystoma tigrinum* virus eukaryotic translation initiation factor 2 α homologue. *Journal of Virology*, 85(10), 5061–5069. <https://doi.org/10.1128/JVI.01488-10>
- Jancovich, J. K., Mao, J., Chinchar, V. G., Wyatt, C., Case, S. T., Kumar, S., Valente, G., Subramanian, S., Davidson, E. W., Collins, J. P., & Jacobs, B. L. (2003). Genomic sequence of a ranavirus (family Iridoviridae) associated with salamander mortalities in North America. *Virology*, 316(1). <https://doi.org/10.1016/j.virol.2003.08.001>
- Johnson, K. A., & Goody, R. S. (2011). The Original Michaelis Constant: Translation of the 1913 Michaelis–Menten Paper. *Biochemistry*, 50(39), 8264–8269. <https://doi.org/10.1021/bi201284u>
- Kaushal, S. S., Likens, G. E., Jaworski, N. A., Pace, M. L., Sides, A. M., Seekell, D., Belt, K. T., Secor, D. H., & Wingate, R. L. (2010). Rising stream and river temperatures in the United States. *Frontiers in Ecology and the Environment*, 8(9), 461–466. <https://doi.org/10.1890/090037>
- Keeling, M. J., & Rohani, P. (2007). *Modeling Infectious Diseases in Humans and Animals*. Princeton University Press.
- Lafferty, K. D., & Mordecai, E. A. (2016). The rise and fall of infectious disease in a warmer world. *F1000Research*, 5, 2040. <https://doi.org/10.12688/f1000research.8766.1>
- Lips, K. R., Diffendorfer, J., Mendelson, J. R., & Sears, M. W. (2008). Riding the Wave: Reconciling the Roles of Disease and Climate Change in Amphibian Declines. *PLoS Biology*, 6(3). <https://doi.org/10.1371/journal.pbio.0060072>
- Martinez, M. E. (2018). The calendar of epidemics: Seasonal cycles of infectious diseases. *PLOS Pathogens*, 14(11). <https://doi.org/10.1371/journal.ppat.1007327>

- McPherson, M., García-García, A., Cuesta-Valero, F. J., Beltrami, H., Hansen-Ketchum, P., MacDougall, D., & Ogden, N. H. (2017). Expansion of the Lyme Disease Vector *Ixodes Scapularis* in Canada Inferred from CMIP5 Climate Projections. *Environmental Health Perspectives*, *125*(5), 057008. <https://doi.org/10.1289/EHP57>
- Mihaljevic, J. R., Greer, A. L., & Brunner, J. L. (2019). Evaluating the Within-Host Dynamics of Ranavirus Infection with Mechanistic Disease Models and Experimental Data. *Viruses*, *11*(5). <https://doi.org/10.3390/v11050396>
- Mihaljevic, J. R., Polivka, C. M., Mehmel, C. J., Li, C., Dukic, V., & Dwyer, G. (2020). An Empirical Test of the Role of Small-Scale Transmission in Large-Scale Disease Dynamics. *The American Naturalist*, *195*(4). <https://doi.org/10.1086/707457>
- Molnár, P. K., Kutz, S. J., Hoar, B. M., & Dobson, A. P. (2013). Metabolic approaches to understanding climate change impacts on seasonal host-macroparasite dynamics. *Ecology Letters*, *16*(1), 9–21. <https://doi.org/10.1111/ele.12022>
- Munro, J., Bayley, A. E., McPherson, N. J., & Feist, S. W. (2016). Survival of Frog Virus 3 in Freshwater and Sediment from an English Lake. *Journal of Wildlife Diseases*, *52*(1), 138–142. <https://doi.org/10.7589/2015-02-033>
- Pearman, P. B., & Garner, T. W. J. (2005). Susceptibility of Italian agile frog populations to an emerging strain of Ranavirus parallels population genetic diversity. *Ecology Letters*, *8*(4), 401–408. <https://doi.org/10.1111/j.1461-0248.2005.00735.x>
- Raffel, T. R., Rohr, J. R., Kiesecker, J. M., & Hudson, P. J. (2006). Negative effects of changing temperature on amphibian immunity under field conditions. *Functional Ecology*, *20*(5). <https://doi.org/10.1111/j.1365-2435.2006.01159.x>
- Ridenhour, B. J., & Storfer, A. T. (2008). Geographically variable selection in *Ambystoma tigrinum* virus (Iridoviridae) throughout the western USA. *Journal of Evolutionary Biology*, *21*(4). <https://doi.org/10.1111/j.1420-9101.2008.01537.x>
- Robert, J., George, E., de Jesús Andino, F., & Chen, G. (2011). Waterborne infectivity of the Ranavirus frog virus 3 in *Xenopus laevis*. *Virology*, *417*(2), 410–417. <https://doi.org/10.1016/j.virol.2011.06.026>
- Rohr, J. R., Raffel, T. R., Romansic, J. M., McCallum, H., & Hudson, P. J. (2008). Evaluating the links between climate, disease spread, and amphibian declines. *Proceedings of the National Academy of Sciences*, *105*(45). <https://doi.org/10.1073/pnas.0806368105>
- Rojas, S., Richards, K., Jancovich, J. K., & Davidson, E. W. (2005). Influence of temperature on Ranavirus infection in larval salamanders *Ambystoma tigrinum*. *Diseases of Aquatic Organisms*, *63*(2–3). <https://doi.org/10.3354/dao063095>
- Rosenbaum, B., & Rall, B. C. (2018). Fitting functional responses: Direct parameter estimation by simulating differential equations. *Methods in Ecology and Evolution*, *9*(10), 2076–2090. <https://doi.org/10.1111/2041-210X.13039>

- Samanta, M., Yim, J., de Jesús Andino, F., Paiola, M., & Robert, J. (2021). TLR5-Mediated Reactivation of Quiescent Ranavirus FV3 in *Xenopus* Peritoneal Macrophages. *Journal of Virology*, 95(12). <https://doi.org/10.1128/JVI.00215-21>
- Schock, D. M., Bollinger, T. K., & Collins, J. P. (2009). Mortality Rates Differ Among Amphibian Populations Exposed to Three Strains of a Lethal Ranavirus. *EcoHealth*, 6(3), 438–448. <https://doi.org/10.1007/s10393-010-0279-0>
- Stilwell, N., Whittington, R. J., Hick, P., Becker, J. A., Ariel, E., Van Beurden, S., Vendramin, N., Olesen, N., And Waltz (2018). Partial Validation Of A Taqman Real-time Quantitative PCR For The Detection Of Ranaviruses. *Diseases Of Aquatic Organisms*, 128:105–116.
- Tornabene, B. J., Blaustein, A. R., Briggs, C. J., Calhoun, D. M., Johnson, P. T. J., McDevitt-Galles, T., Rohr, J. R., & Hoverman, J. T. (2018). The influence of landscape and environmental factors on ranavirus epidemiology in a California amphibian assemblage. *Freshwater Biology*, 63(7). <https://doi.org/10.1111/fwb.13100>
- van Buskirk, J., & Smith, D. C. (1991). Density-Dependent Population Regulation in a Salamander. *Ecology*, 72(5), 1747–1756. <https://doi.org/10.2307/1940973>
- Vilaça, S. T., Bienentreu, J.-F., Brunetti, C. R., Lesbarrères, D., Murray, D. L., & Kyle, C. J. (2019). Frog Virus 3 Genomes Reveal Prevalent Recombination between Ranavirus Lineages and Their Origins in Canada. *Journal of Virology*, 93(20). <https://doi.org/10.1128/JVI.00765-19>